Reprogramming of the cardiac phosphoproteome in conjunction with proteome and transcriptome creates the enhanced performance and protection circuitry in response to chronic adenylyl cyclase-driven stress

Jia-Hua Qu, Khalid Chakir, Kirill V. Tarasov, Daniel R. Riordon, Maria Grazia Perino, Allwin Jennifa Silvester, and Edward G. Lakatta *

Laboratory of Cardiovascular Science, Intramural Research Program, National Institute on Aging, National Institutes of Health, Baltimore, MD 21224, USA.

Address correspondence to:

Dr. Edward G. Lakatta*

Laboratory of Cardiovascular Science

Intramural Research Program

National Institute on Aging

National Institutes of Health

251 Bayview Boulevard

Suite 100

Baltimore, MD 21224

USA.

Tel: +1 410-558-8202

lakattae@grc.nia.nih.gov

Abstract

Our previous work demonstrated the existence of a remarkable adaptive paradigm of heart performance and protection in response to the constitutive challenge of marked cardiac-specific overexpression of adenylyl cyclase type 8 (TGAC8), based on transcriptome and proteome. Because PKA signaling is the predominantly activated pathway in the TGAC8 left ventricle (LV) performance and protection circuitry, we hypothesized that phosphorylation states of numerous proteins are increased in pathways in which the transcriptome and proteome were activated TGAC8 vs. WT. We conducted an unbiased phosphoproteomics analysis in order to determine the role of altered protein phosphorylation in the chronic adaptive heart performance and protection profile of adult TGAC8 LV at 3-4 months of age. We identified 12,963 phospho-peptides and 3646 phosphoproteins, including 4990 upregulated phosphopeptides and 781 differentially regulated (741 Up and 40 Down) phosphoproteins in TGAC8 vs. WT. Based on differentially regulated phosphoproteins by genotype, numerous stress response canonical pathways within reprogrammed TGAC8 LV, including protein kinase A (PKA) signaling, PI3K signaling, and AMPK signaling, predicted upstream regulators, e.g., PDPK1, PAK1 and PTK2B, and downstream functions, e.g., cell viability, protein quality control, and metabolism were enriched. In addition to PKA, numerous kinases (83) and phosphatases (30) were hyper-phosphorylated in TGAC8 vs. WT. Hyper-phosphorylated transcriptional factors in TGAC8 were associated with increased mRNA transcription, and immune responses and metabolism pathways. Combining the phosphoproteome with its proteome and with the previously published TGAC8 transcriptome enabled the elucidation of which cardiac performance and adaptive protection profiles were coordinately regulated at post-translational modification (PTM) (phosphorylation), translational and transcriptional levels. Many stress response signaling pathways, i.e., PI3K/AKT, ERK/MAPK and ubiquitin labeling, were consistently enriched at transcriptional, translational and PTM levels, and that PI3K/AKT and ERK/MAPK signaling pathways were also activated in the TGAC8 LV. We verified some results via western blot and protein synthesis and degradation detection experiments. Thus, PTM of protein by phosphorylation, per se, contributes immensely to the heart performance and protection profile of TGAC8 LV, and is coordinately regulated with altered transcription and translation in the TGAC8 to activate critical stress response pathways.

Keywords

left ventricle, adenylyl cyclase 8, AC-cAMP-PKA-Ca^{2+} signaling, phosphoproteome, proteome, transcriptome, PI3K/AKT signaling pathway.

Introduction

Cyclic AMP (cAMP) is a pivotal second messenger, which exerts multifaceted effects on most significant physiological processes, such as cardiac contractility, glycogenolysis and lipolysis, hormone release, etc[1]. In mammalians, there are nine transmembrane adenylyl cyclase (AC) (mAC) isoforms (AC1-9) and one soluble AC (sAC, also called AC10) catalyzing the conversion

of ATP into cAMP[2], which usually activates the phosphorylation cascade, serving as the central motif of cellular signaling[1,3]. Increased AC-cAMP-PKA-Ca^{2+} signaling is the quintessential component of both acute and chronic cardiac responses.

AC8, the isoform, is highly expressed in brain regions[2,4]. Unlike two dominant cardiac AC isoforms, AC5 and AC6, which are inhibited by intracellular Ca^{2+} and inhibited in heart failure (HF), AC8 is stimulated by Ca^{2+}-calmodulin (CM)[5,6] and involved in nervous system functions, like learning and memory[2,4]. Our lab and others have demonstrated that cardiac-specific overexpression of AC8 (TGAC8) markedly increases the heart rate and ejection fraction, similar to acute exercise but chronic and in the absence of corporal exertion, and persists on a 24 hours per day and 7 days per week basis[5,7-9]. Despite this persistent high-level of heart performance driven by markedly elevated level of AC8-cAMP -PKA-Ca^{2+} signaling, which usually proceeds to near-term cardiac dysfunction, the TGAC8 survives for an extended period of time, up to about a year of age without excessive mortality.

It is of utmost importance to unravel how the TGAC8 adapts the heart to this chronic stress, as this knowledge can be applied to the study of cardiac physiology and pathology and even to develop treatments for cardiovascular diseases (CVDs). In this regard, as a first "port-of-call", we had recently compared the LV transcriptome and proteome in TGAC8 and WT littermates[10]. Because PKA signaling pathway was highly enriched in TGAC8 vs. WT, we reasoned that protein phosphorylation will differ between TGAC8 and WT, and the phosphorylation modification will play a crucial role in the remarkable adaptation capacity of the TGAC8 heart in response to markedly increased AC8-cAMP-PKA-Ca^{2+} signaling. We have assessed the concordance of the genotypic differences at the phosphorylation level to some degree in western blot (WB) experiments[10].

As the body is a quite complex system, regulation at a single level cannot reveal the whole picture in an organism, and multiple levels of regulatory mechanisms are coordinated to defend against stimuli and maintain health[11]. Phosphorylation is one of the most important and most extensively studied post-translational modifications (PTMs) on proteins. Various kinases and phosphatases within cells phosphorylate and dephosphorylate a myriad of proteins respectively to regulate their activities and affect multiple signaling pathways. In the present research, we conducted Tandem Mass Tag (TMT)-labeling MS of left ventricular samples of the three-month old male TGAC8 and WT mice, to unravel the reprogrammed phosphoproteome and proteome of the TGAC8 left ventricle (LV). In addition, by comparing genotypic differences in the proteome and phosphoproteome of the present study with genotypic differences in transcriptome published previously[10], we sought to determine whether some adaptive mechanisms that emerge in the TGAC8 LV are regulated at transcriptional, translational and PTM (phosphorylation) levels.

Materials and Methods

1. Animals.

The cardiac-specific overexpression of AC8 (TGAC8) mouse, generated by inserting a cDNA coding for human AC8 after the murine α-myosin heavy chain promoter, was a gift from Nicole Defer/Jacques Hanoune, Unite de Recherches, INSERM U-99, Hôpital Henri Mondor, F-94010 Créteil, France. The 12-week old male TGAC mice were used as study cases, and age matched WT littermates, in the C57/BL6 background, were used as controls. All studies were performed in accordance with the Guide for the Care and Use of Laboratory Animals published by the National Institutes of Health (NIH Publication no. 85-23, revised 1996). The experimental protocols were approved by the Animal Care and Use Committee of the National Institutes of Health (protocol #441-LCS-2016).

2. Isolate and store mouse heart.

Three-month old male C57 mice (TGAC8 and WT) were euthanized and the heart was isolated. The left ventricle (LV) tissues were extracted and stored in tubes at -80°C.

3. Mass spectrometry for phosphoproteome and data process.

Four TGAC8 LVs and five WT LVs were sent to National Heart, Lung, and Blood Institute, National Institutes of Health, Bethesda to conduct mass spectrometry using the standard tandem mass tag (TMT) labeling method to obtain the phosphoproteome and total proteome concurrently in the same platform. The raw data were processed in Proteome Discover (ThermoFisher Scientific, software version 2.2). After filtering low quality signal, we remained the medium and high confidence peptides. For total proteins and phosphoproteins, we combined peptides to computed the normalized/standardized expressions with the default parameters. Then we divided the expressions of phosphoproteins to those of total proteins to obtain the normalized phosphoproteome. As the expressions appeared to be near normal distribution, we calculated the fold change by dividing the average value of TGAC8 samples by the average value of WT samples, and calculated p-value using two-sided unpaired Student's t-test.

4. Analyses of the TGAC8 LV transcriptome.

The processed transcriptomic data were obtained from our recently published work (ref). The significantly changed mRNAs (TGAC8 vs. WT, q-value < 0.05) were uploaded into DAVID[2] (version: 6.8; https://david.ncifcrf.gov/home.jsp) for Gene Ontology (GO) term enrichments, and were also imported into Ingenuity Pathway Analysis[3] (IPA (QIAGEN, March 2020)) for upstream kinases and phosphatases prediction. Kinases and phosphatases were selected from the

132 transcriptome and their changes at mRNA level were displayed to observe their regulation by the
133 overexpression of AC8.

134

135 **5. Analyses of phosphoproteome.**

136 Both unnormalized and normalized phosphoproteome were analyzed and visualized in PCA,
137 heatmap, and volcano plots. With the cutoff -log(p-value) > 1.3 and absolute(log2(fold change))
138 ≥ 0.4, we obtained the significantly changed unnormalized and normalized phosphoproteins
139 (TGAC8 vs. WT) and imported them into IPA for functional analyses respectively, and
140 compared the canonical pathway enrichments from these two datasets. In IPA, the upstream
141 kinases were predicted based upon the unnormalized phosphoproteom, and the regulatory
142 pathways from the predicted upstream kinases to downstream effective signaling pathways were
143 generated. Molecular and cellular functions were also enriched in IPA. The similar analyses to
144 those conducted in the TGAC8 LV transcriptome were also done in the TGAC8 LV total
145 proteome to observe the GO term enrichment, predicted activities of upstream kinases and
146 phosphatases, and expression of kinases and phosphatases at protein level.

147

148 **6. Analyses of phosphopeptides.**

149 The upregulated phosphopeptides (TGAC8 vs. WT, p-value < 0.05 and log2(fold change) > 0)
150 were processed in R. After split of peptides with multiple phosphosites into individual peptides
151 and filtration of ambiguously identified sites, 2264 phosphopeptides were selected. Protein
152 peptide sequences of full length were downloaded from Uniprot database[12] and matched to the
153 protein accessions corresponding to processed and selected phosphopeptides. Peptides centered
154 on the phosphosites and flanked by 6 amino acids on the N and C termini respectively were
155 extracted from the matched protein peptide sequences, and uploaded into WebLogo[13]
156 (http://weblogo.threeplusone.com/) and iceLogo[14] (https://iomics.ugent.be/icelogoserver/) for
157 sequence motif analysis. In WebLogo online analysis, different amino acids were labeled in
158 different colors representing different chemical properties (refer to figure legend). In iceLogo
159 online analysis, a public amphiphilicity index of polar amino acids reported by Mitaku and
160 colleagues[15] was used as an aid to characterize the amino acid preference at membrane-water
161 interfaces. In addition, the phosphopeptides of PI3K/Akt substates were summarized and
162 displayed in stacked bar plots.

163

164 **7. Integrative analyses of transcriptome, proteome and phosphoproteome.**

165 The changes of significantly regulated molecules (TGAC8 vs. WT, q-value or p-value < 0.05) in
166 transcriptome, total proteome, and unnormalized phosphoproteome were displayed in circos plot.
167 In addition, the changes at different level were compared and visualized in correlation scatter

plots. The discordant proteins whose changes directions in total proteome and phosphoproteome were opposite were used to analyze the specific regulation at the phosphorylation level by the use of Reactome and GO (Cellular component and biological process) databases.

As to the coordinated regulation, the above mentioned significantly regulated molecules (TGAC8 vs. WT) in each dataset were imported into IPA for canonical pathway enrichment. PI3K/AKT signaling and protein ubiquitination were two coordinated pathways across all omics. The phosphopeptides of protein substrates of PI3K were extracted from the phosphopeptide dataset and the numbers of changed phosphopeptides (TGAC8 vs. WT) were summarized and visualized in stacked bar plot. The PI3K/AKT signaling pathway were visualized in IPA, and nodes in the pathways were marked in different colors in terms of their changes at different levels.

As kinases and phosphatases are pivotal in phosphorylation, and transcription factors (TFs) are important in transcription regulation, they were extracted from transcriptome, proteome, and phosphoproteome to observe their changes (TGAC8 vs. WT) and deduce their role in the reprogram of phosphoproteome. The upstream transcription regulators including but not only TFs were predicted on the basis of transcriptome and proteome by the utilization of knowledge base in IPA, and their expressions were searched in multiple datasets. Furtherly, TFs that were significantly regulated at phosphorylation level (TGAC8 vs. WT, $p\text{-value} < 0.05$) were defined as significantly changed phosphorylated TFs in this research, and they were uploaded into STRING database[4] (version: 11.0; http://string-db.org/) to generate protein-protein interaction network and enrich KEGG pathways. They were also imported into IPA for canonical pathway, molecular and cellular functions enrichments.

8. Data process and graphics production.

Most raw data were precleared and processed using RStudio (version: 1.1.463) in R language (version: 3.5.3), in which the tidyr package and dplyr package were applied. In addition, GraphPad Prism (version: 7), Microsoft Excel (version: 2019) and Adobe Illustrator (version: CC 2019) were also used for statistics and graphics. Venn diagrams were generated in Venny[5] (version: 2.1.0; http://bioinfogp.cnb.csic.es/tools/venny/index.html). Circos plot was generated using Circos software[6] in Perl language.

Results

1. The TGAC8 reprograms the LV phosphoproteome.

202 The TMT-labeling quantitative MS identified **12,963 phospho-peptides** (File 1: Sheet 1) and
203 **3646 phosphoproteins** (File 1: Sheet 2). The principal component analysis (PCA) (Figure 1A)
204 of the 3646 phosphoproteins in each mouse showed that the TG and WT samples were
205 distinguished into two groups completely. The heatmap (Figure 1B) showed the intra-group
206 consistency of upregulated phosphoproteins in TGAC8 compared to WT. Within the cutoff at -
207 log10(p-value) > 1.3 and absolute value of log2(fold-change(TG/WT)) ≥ 0.04, 781
208 phosphoproteins were differentially regulated by genotype. Of the 781 phosphoproteins, the
209 phosphorylation levels of 741 proteins were increased and only 40 were decreased in the TGAC8
210 vs. WT LV (Figure 1C).

211

212 **2. Functional analyses of the phosphoproteome.**

213 We performed the canonical pathway, upstream regulation, and downstream function analyses of
214 the remodeled LV phosphoproteome of TGAC8 using the Ingenuity Pathway Analysis (IPA)
215 software.

216 **2.1. Canonical pathway analysis of the remodeled LV phosphoproteome of TGAC8.**

217 To study the mechanism at phosphorylation level, we first performed canonical pathway analysis
218 using IPA. Top canonical pathways within the phosphoproteome that were statistically
219 differentially enriched in TGAC8 vs. WT were displayed in the bar plot (Figure 1D and File 2:
220 Sheet 1). Of these pathways, cardiac hypertrophy signaling (enhanced) is most highly activated
221 (z-score as high as 4.867) (Figure 1D). The combination of Supplementary Figure 1 and File 2:
222 Sheet 2 and our recently published work[10] showed that the phosphorylation status of numerous
223 molecules, e.g., Ca^{2+} ATPase, RyR2, Ncx, involved in excitation, calcium cycling, contraction,
224 relaxation and protein synthesis, was elevated in the TGAC8 vs. WT LV. However, we have
225 demonstrated that at three-month of age, the mouse age in the present study, the LV mass is not
226 elevated in TGAC8 vs. WT[10]. Of note, transcriptomic, proteomic and WB analyses indicated that
227 pathologic hypertrophic markers were not increased in TGAC8 vs. WT[10]. In this regard, the
228 activation of key stress response signaling pathways, e.g., protein kinase A (PKA) signaling,
229 PI3K signaling, and AMPK signaling, may protect against pathological changes, that result in an
230 increase in cardiac mass in TGAC8 despite its chronic increase in performance. For example,
231 activated PKA signaling can restrict the activity of AC8, acting as a feedback to fine-tune the
232 downstream signaling networks inside the body[3]. Additionally, nitric oxide (NO) signaling may
233 coordinate cardiac protection in the increase in cardiac mass (Figure 1D). Increased
234 phosphorylation status of HSP90 and Akt in TGAC8 synergistically increase eNOS activity[16],
235 and increased NO produced by eNOS may modulate the function of the ryanodine receptor Ca^{2+}
236 release channel (RyR2), which was increased on the PKA dependent phosphopeptides in
237 TGAC8, on the cardiac sarcoplasmic reticulum[17]. The TMT-labeling MS identified significant
238 upregulated phosphorylation in the peptides of RyR2 (RISQTSQVSIDAAHGYSPR, E9Q401

239 [2805-2823]) (File 1: Sheet 1) , consistent with the PKA induced phosphorylation of RyR2-
240 S2809 mediating the increase in Ca^{2+} spark amplitude[18].

241 **2.2. Upstream regulators of the remodeled LV phosphoproteome of TGAC8.**

242 As known, the overexpression of AC8 activates the AC8-cAMP-PKA phosphorylation axis[9].
243 There were 2264 phosphosites whose names and locations are unambiguous within the 4990
244 upregulated phosphopeptides (p-value ≤ 0.05 and log2(fold-change(TG/WT)) ≥ 0) in TGAC8 vs.
245 WT. The majority of these phosphosites were serines (S) and threonines (T), and a few were
246 tyrosines (Y) (Figure 2A). By using WebLogo, we profiled the phosphorylation motif sequences
247 (Figure 2B). A typical PKA and AKT substate motif, R-R-X-pS/T, was the most abundant
248 substrate motif, consistent with increased PKA dependent phosphorylation (Figure 2B-2D)[19,20].
249 In addition to S and T, the center phosphosites also included phosphotyrosine (Y). The center
250 phosphosites were mainly flanked by the P-E-E sequence on the C terminus, endowing a strong
251 hydrophobic and acidic property to the C terminus of the substrate sequences (Figure 2B),
252 supported by the amphiphilicity index analysis in iceLogo (Figure 2E). Because phosphorylation
253 substrate motifs were not restricted to PKA's substrate motif, additional kinases must be also
254 involved in reprogramming the TGAC8 phosphoproteome. Therefore, we were inspired to
255 explore additional kinase-substrate pathways mediating the effect of the cardiac-overexpression
256 of AC8 here.

257 IPA predicted that 26 kinases were responsible for the above-mentioned phosphorylation motifs
258 (File 2: Sheet 3), among which, three had previously been identified to differ by genotype in the
259 LV transcriptome, 18 were previously shown to differ by genotype in the LV proteome, and 18
260 were identified in the present phosphoproteome. Of note, most of the identified kinases were
261 upregulated in TGAC8 vs. WT at transcription, translation and PTM (phosphorylation) levels.
262 Within the phosphoproteome, eight kinases were predicted to be differentially activated by
263 genotype, and the phosphorylation level of four of these (PDPK1, PAK1, PTK2B and GSK3B)
264 was increased in TGAC8 vs. WT. These four kinases each phosphorylates various proteins to
265 regulate cellular functions. For example, a previous study observed that in human glioblastoma
266 cell lines, T98G and U87MG cells, the interference of human PDPK1 mRNA by siRNA
267 decreased the phosphorylation level of human BAD protein (S112, S136 and S155) and activated
268 cell death to suppress tumorigenesis[21]. Another study reported that in mouse myoblast cell line,
269 C2C12 cells, PDPK1 protein phosphorylated the mouse ULK1 protein[22]. Increased
270 phosphorylation states of BAD (upregulated at S112, S136 and S155) and ULK1 (upregulated at
271 S450, S521 and S637/638) in TGAC8 may be linked to activated PDPK1.

272 Different kinases can coordinate to reprogram the complex regulation network in the organism.
273 Consistent with the IPA canonical pathway analysis, the phosphorylation level of 27 proteins
274 (including the three kinases (PDPK1, PAK1 and PTK2B) auto-phosphorylating themselves)
275 were elevated by the three kinases to regulate cardiac stress signaling pathways, including PKA
276 signaling, ERK/MAPK signaling, cardiac hypertrophy signaling (enhanced), and renin-

277 angiotensin signaling (Figure 1E), to cope with the cardiac stress in the TGAC8. For example,
278 GSK3B is involved in multiple biological processes. PDPK1 phosphorylated GSK3B at S9[23,24]
279 and PTK2B phosphorylated GSK3B at S9 and Y216[25,26] to inhibit the kinase activity of GSK3B.
280 In this phosphoproteome, GSK3B was phosphorylated at multiple sites, including S9, Y216,
281 S219 and S545, and thus GSK3B inhibition was linked to the cardiac adaptation[27,28].

282 **2.3. Downstream functions of the remodeled LV phosphoproteome of TGAC8.**

283 To study the downstream functions of these phosphoproteins, we performed molecular and
284 cellular functions analysis in IPA. The enriched functions were mainly in three categories, i.e.,
285 cell viability, protein quality control, and metabolism (Figure 1F and File 2: Sheet5). The
286 functions of cellular assembly and organization, cellular function and maintenance, and cell
287 death and survival were ranked as the top three terms, indicating the important role of the
288 reprogrammed phosphoproteome in improving cell viability in response to the chronic stress of
289 the overexpression of AC8 in the mouse heart.

290

291 **3. Integrative analyses of transcriptome, proteome and phosphoproteome.**

292 We next integrated changes in PTM (phosphorylation) in TGAC8 vs. WT with genotypic
293 differences in protein translation and in transcription. The circos plot (Figure 3A) illustrates the
294 genotypic differences (TGAC8 vs. WT) in **molecules** identified across the transcriptome,
295 proteome, and phosphoproteome. In addition, the correlation scatter plots (Figure 3B)
296 demonstrated a moderate level of correlation of genotypic differences of molecular changes
297 within phosphoproteome and transcriptome, and a somewhat stronger correlation between
298 genotypic differences of molecular changes within phosphoproteome and proteome (Figure 3C).
299 Concordant and discordant enrichments of canonical pathways differed by genotype among the
300 three omics are shown in Figure 3D. A comparison of genotypic differences within the three
301 omics highlights the importance of protein phosphorylation, and the phosphorylation was
302 **coordinated with and supplemental to** transcription and translation.

303 Because kinases and phosphatases are the key regulators of phosphorylation, and
304 phosphorylation of transcriptional factors (TFs) are the primary determinant of their activities in
305 transcription, we compared genotypic differences in kinases, phosphatases and TFs within the
306 phosphoproteome and proteome with our previously published genotypic differences in the
307 TGAC8 vs. WT transcriptome[10] (Figure 3E). We identified 196 kinases, 71 phosphatases and
308 191 TFs in the present phosphoproteome (Figure 3F). The protein phosphorylation status of
309 about one half of these molecules differed significantly (p-value < 0.05) by genotype (Figure
310 3G), and the protein phosphorylation status of majority of these molecules was increased (Figure
311 3H-3J). The genotypic differences in the transcription (mRNA expression obtained from RNA-
312 seq) and translation (protein expression obtained from mass spectrometry) of these molecules,
313 however, differed from those in the phosphoproteome (Figure 3E). Because there were more

molecules that were unchanged or reduced in the TGAC8 vs. WT transcriptome or proteome than in the phosphoproteome, it is clear that the changes in protein phosphorylation are of utmost importance in the coordination of transcription, translation and PTM, that underlie the adaptive response of the TGAC8 LV to the marked, chronic increase stress of its intrinsically activated AC-cAMP-PKA-Ca^{2+} signaling. Thus, by utilizing multiple bioinformatic analysis methods, we not only dissected the reprogrammed phosphoproteome and deduced its functions in the TGAC8 mouse LV, but also profiled the coordination of phosphoproteome, transcriptome and proteome.

3.1. Implications of coordinated changes in protein phosphorylation and transcription in TGAC8 vs. WT.

The most likely type of coordination between protein phosphorylation and transcription is related to phosphorylation states of TFs which is determined by kinases and phosphatases activities. Analysis of the remodeled LV transcriptome of TGAC8 in Gene Ontology (GO) analysis using DAVID online software discovered that enrichments of numerous phosphorylation and dephosphorylation related biological processes and molecular functions significantly differed by genotype (Figure 4A), and that the coordinated expression of numerous kinases and phosphatases also differed by genotype (Figure 4B-4C and File 8). Because expression levels of kinases and phosphatases do not denote their activation states, we utilized IPA to predict the genotypic differences in activation states of upstream kinase and phosphatase (regulators of the transcriptome). Intriguingly, 60 kinases were predicted to be upstream regulators of the remodeled LV transcriptome of TGAC8, and the majority of these kinases were predicted to be activated in TGAC8 vs. WT (Figure 4D and File 9). In contrast, many fewer phosphatases were predicted between TGAC8 and WT, and most of these were predicted to be inhibited (Figure 4E and File 9). Thus, the differential genotypic enrichment of phosphorylation status and predicted activation of kinases and phosphatases identified in our post hoc analysis of our previously reported TGAC8 vs. WT transcriptome[10] are linked to the differential genotypic reprogramming of the phosphoproteome discovered in the present study.

We utilized IPA to predict the activation states of upstream transcription regulators on the basis of the remodeled LV transcriptomes and proteomes, and then determined their expression levels in transcriptome, proteome and phosphoproteome (Figure 4F). Because TFs are the main regulators of transcription, and because phosphorylation of TFs usually regulates their activities[29-31], we focused our subsequent analysis on functions of those TFs that were differentially phosphorylated in TGAC8 vs. WT. To confirm the hypothesis that the TGAC8 might exert transcriptional control by TFs phosphorylation, we retrieved all TFs identified in our previous transcriptome and proteome[10] and mapped them to the current phosphoproteome in order to determine their genotypic differences in phosphorylation status. Of the 191 TFs also identified in this phosphoproteome, 92 TFs differed significantly by genotype in phosphorylation status (p-value < 0.05). In agreement with the general upregulated transcription in TGAC8 LV[10], nearly all of the TF that differed by genotype had increased phosphorylation level (Figure 4G

352 and File 3). The only exception was purine rich element binding protein G (Purg), known to be
353 hyper-phosphorylated in solid tumors[32].

354 We conducted Kyoto Encyclopedia of Genes and Genomes (KEGG) pathway analysis to further
355 probe the predicted facts of TFs that were generally hyper-phosphorylated in TGAC8 vs. WT.
356 Numerous immunity related pathways, cancer related pathways, and metabolism related
357 pathways were enriched (Figure 4H and File 4). We then utilized IPA for in-depth analysis.
358 Numerous metabolic canonical pathways (glucocorticoid receptor signaling and PPAR
359 signaling), a cancer related canonical pathway (regulation of epithelial-mesenchymal transition
360 pathway), and immunity related canonical pathways (role of JAK1, JAK2 and TYK2 in
361 interferon signaling, IL-9 signaling, JAK/Stat signaling, etc.) were enriched (Figure 4I and File
362 5: Sheet 1). Intriguingly, the sumoylation pathway was markedly inhibited. Because both
363 sumoylation and phosphorylation are important PTMs in transcriptional regulation[33,34], it is
364 possible that the upregulated protein phosphorylation and inhibited protein sumoylation pathway
365 in TFs coordinately activate transcription and improve immunity in the TGAC8 LV. In addition,
366 cell viability and metabolism in molecular and cellular functions were enriched in TGAC8 vs.
367 WT (Figure 4J and File 5: Sheet 2), consistent with enrichments of afore mentioned KEGG
368 pathways and IPA canonical pathways (Figure 4H and 4I).

369 Taken together, we have discovered the existence of substantial crosstalk between protein
370 phosphorylation and transcription in the TGAC8 LV: phosphorylation of TFs reprograms
371 immunity and metabolism pathways and functions in the TGAC8 LV, likely serving to maintain
372 cell survival in response to the chronic stress of marked AC8 overexpression.

373 **3.2. Coordinated changes in protein expression and phosphorylation of the remodeled**
374 **proteome and phosphoproteome of TGAC8.**

375 Having discovered the coordinated changes in the remodeled TGAC8 transcriptome and
376 phosphoproteome (Figure 4A-4E), we next sought to discover the extent to which changes in the
377 remodeled phosphoproteome of the TGAC8 LV were coordinated with changes in its remodeled
378 proteome. Numerous biological processes and molecular functions that were related to
379 phosphorylation and dephosphorylation were enriched in the remodeled TGAC8 LV proteome
380 (Figure 5A), as were numerous kinases and phosphatases (Figure 5B-5C and File 10). Twenty-
381 nine kinases that differed by genotype were predicted to be upstream regulators of the proteome,
382 and most of these were predicted to be activated in TGAC8 vs. WT. Fewer phosphatases than
383 kinases that differed by genotype were identified as upstream regulators of the remodeled
384 TGAC8 LV proteome (Figure 5D-5E and File 11).

385 One strategy adopted to probe deeper into the coordinated changes in the proteome and
386 phosphoproteome of the TGAC8 LV was to normalize the phosphoproteome to the total
387 proteome (in other words, to divide the phosphorylation expression by protein expression) (File
388 1: sheet4). Of the 3927 phosphoproteins identified in our mouse LV samples, 2164 were
389 identified in both the proteome and phosphoproteome, and these were focused for subsequent

390 analyses. After normalization, WT and TGAC8 samples manifested clear genotypic differences
391 in PCA analysis (Figure 5G), and phosphorylation status of numerous proteins normalized to the
392 protein expression level still differed by genotype without cutoff (Figure 5H) and with cutoff (-
393 log(p-value) > 1.3 and absolute(log2(TG/WT)) ≥ 0.4) (Figure 5I). Even after normalizing the
394 phosphorylation level to the protein expression level, the enrichments of canonical pathways in
395 TGAC8 were quite consistent with those of unnormalized phosphoproteome (Figure 5J and File
396 6). Cardiac hypertrophy signaling (enhanced) and cardiac hypertrophy signaling took the top two
397 places, emphasizing the important role of phosphorylation in the regulation of cardiac functions
398 in response to chronic stress when coordinated with changes in the total proteome.

399 Many important stress-response signaling pathways were enriched from phosphoproteome, e.g.,
400 PKA signaling, ERK/MAPK signaling, insulin receptor signaling, and PI3K/AKT signaling
401 (Figure 6A). Three of these pathways, PI3K/AKT, ERK/MAPK and ubiquitin labeling, were also
402 markedly enriched in our previous analysis on total proteome in TGAC8 LV^{35}. By integrating
403 and comparing the enrichments from transcriptome, proteome and phosphoproteome, we were
404 able to identify the three signaling pathways in the TGAC8 LV, PI3K/AKT, ERK/MAPK and
405 ubiquitin labeling, that were regulated concordantly in transcription, translation, and PTM
406 (phosphorylation) (Figure 6B). PI3K/AKT and ERK/MAPK signaling pathways are not only
407 enriched but also activated in TGAC8. We verified the phosphorylation and activation of
408 PI3K/AKT (Figure 6E and 7A) and ERK/MAPK (Figure 7B-7C) signaling pathways via WB.
409 Their activations are crucial for the increase in protein synthesis and cell survival in the TGAC8
410 LV^{35}. Protein ubiquitination is an important process in protein degradation, which is also
411 increased in TGAC8 LV^{35}, but the activity of this pathways could not be predicted on the basis
412 of present knowledge base of IPA. Therefore, we conducted wet lab experiments. The rate of
413 protein synthesis was 40% higher in TGAC8 than in WT (Figure 7D). The overall ubiquitination,
414 which labels proteins to be degraded, was increased in TGAC8 vs. WT (Figure 6F), and the
415 proteosome activity, which helps to limit the increased protein load of TGAC8 hearts, was also
416 increased in TGAC8 vs. WT (Figure 7E). Therefore, although there was a significant increase in
417 the amount of soluble misfolded proteins in the TGAC8 LV (Figure 7F), insoluble protein
418 aggregates did not accumulate within the TGAC8 LV (Figure 7G). Our experiment results
419 confirmed the enhanced protein synthesis and degradation to improve the proteasome.

420 We next sought to identify which molecules linked to PI3K/AKT signaling differed in TGAC8
421 vs. WT. Among the significantly changed upstream molecules, the majority were upregulated.
422 AKT, a central molecule in the pathway, was also increased in proteome and phosphoproteome
423 (Figure 6C). By searching and mapping the substrates of AKT, we unraveled that the
424 phosphorylation levels of AKT peptide substrates were mostly elevated in TGAC8 vs. WT
425 (Figure 6D and Supplementary Figure 3). Therefore, the downstream effects and functions of
426 AKT signaling were activated in TGAC8 LV: (1) upregulating GSK3 to improve energy
427 metabolism; (2) activating mTOR pathway to increase protein synthesis and cell growth; (3)
428 promoting NF-κB mediated transcription; (4) upregulating BAD and eNOS only at

429 phosphorylational level to enhance cell survival and cardiovascular functions. In summary, to
430 adapt the heart to stress for improved survival, the TGAC8 upregulates the protein
431 phosphorylation to reprogram the cardiac LV phosphoproteome.

432

433 **4. Discordant regulation of the phosphoproteome and proteome in TGAC8 LV.**

434 Among the 443 proteins that differed by genotype in both protein phosphorylation and protein
435 expression levels, 33 were changed discordantly at the two levels (in opposite directions, i.e.,
436 upregulated in proteome but downregulated in phosphoproteome, or vice versa) (Figure 8A and
437 File 7: Sheet 1). We uploaded the 33 discordant proteins into STRING online software for
438 functional analyses. The GO_CC (Cellular Component) analysis resulted in many
439 **mitochondrial components**, indicating the involvement of phosphorylated proteins in
440 mitochondria (Figure 8B and File 7: Sheet 2). Reactome pathway analysis showed that in
441 addition to mitochondria, metabolic pathways were enriched significantly in TGAC8 (Figure 8C
442 and File 7: Sheet 3). Mitochondria are the hub of metabolism and multiple metabolic processes
443 are executed in mitochondria. Consistently, both metabolism and mitochondria related processes
444 were ranked the top processes in GO_BP (Biological Process) analysis (Figure 8D and File 7:
445 Sheet 4). Therefore, the discordant part between total proteome and phosphoproteome indicated
446 that the phosphorylation plays a critical role in the regulation of mitochondria and metabolism in
447 the TGAC8, distinct from its role in regulation at the translational level.

448

449 **5. Deduced schematic of coordination of phosphoproteome with transcriptome and**
450 **proteome in TGAC8 mouse LV.**

451 A deduced schematic integration of the remodeled phosphoproteome, proteome and
452 transcriptome of the TGAC8 LV is shown in Figure 9. The TGAC8 mouse first induces a PKA
453 dependent phosphorylation via AC8-cAMP-PKA axis. Many cytoplasmic proteins including TFs
454 are thus phosphorylated and then transported into the nucleus where TFs recognize and bind to
455 the promoters to activate the transcription of more regulatory factors, including kinases,
456 phosphatases, and TFs. The activation states of these factors are changed upon phosphorylated in
457 cytosol, thereby activating additional kinases-controlled phosphorylation cascades and
458 reprogramming the cardiac phosphoproteome comprehensively.

459

460 **Discussion**

461 Our prior study[35] investigated the adaptive mechanisms that emerge in the TGAC8 heart to
462 marked chronic stress of increased AC8-cAMP-PKA-Ca^{2+} signaling. In that study, a large
463 number of proteins differed in TGAC8 vs. WT. The TGAC8 induced a chronic cardiac exercise
464 phenotype in the heart, i.e., an increase in heart rate and contractility. These functional changes

465 were accompanied by an increased cardiac biomass and energy demand. Multiple signaling
466 pathways, related to nutrient sensing, energy production, cardiac cellular stress, cardiac stress
467 response, growth factor signaling, and cell proliferation, were identified as downstream
468 mediating the effect of the activated AC8-cAMP-PKA-Ca^{2+} signaling in the TGAC8 LV.

469 Our goals here were to determine which proteins in TGAC8 LV differed in expression and
470 phosphorylation status compared to WT, and which kinases/phosphatases play a role in these
471 altered phosphorylation statuses in the TGAC8. By the utilization of TMT-labeling MS, we
472 obtained 12963 phosphopeptides and 3646 phosphoproteins, and observed the general
473 upregulation of phosphorylation. We observed the enrichments of phosphorylation, upregulated
474 expression of kinases, and predicted activation of upstream kinases. We made use of
475 phosphoproteome complementary to transcriptome and proteome to expand our understanding of
476 the regulatory mechanism how the TGAC8 adapts to chronic stress of activated AC8-cAMP-
477 PKA-Ca^{2+} signaling. This approach enabled us to appreciate how changes in the transcription,
478 translation and PTM of proteins in the TGAC8 LV may singly or coordinately enable the
479 TGAC8 to endure the chronic AC8-induced stress (Figure 9).

480 First, the TGAC8 induced a PKA dependent phosphorylation via the AC8-cAMP-PKA axis
481 (typical substrate motif of PKA dependent phosphorylation). Most of previous studies only
482 focused on PKA phosphorylated targets as downstream effects of activated AC8. For example,
483 AC8 induced cAMP activates PKA to increase the phosphorylation of many key proteins in
484 cardiovascular system, e.g., ryanodine-receptor-type 2 (RyR2), L-type Ca^{2+} channels (LTCC),
485 phospholamban (PLN or PLB), etc[36]. In this research, we identified 29 phosphosites on RyR2, 15
486 phosphosites on LTCC alpha 1 and beta 2, and 2 phosphosites (S16 and T17) on PLN, SERCA2
487 and the majority of them were increased in phosphorylation statuses in the TGAC8 LV (File 1:
488 Sheet 1). It is worth noting that PLN is phosphorylated on S16 by PKA whereas on T17 by Ca^{2+}-
489 calmodulin-dependent protein kinase (CaMKII)[37].

490 After the activation of phosphorylation cascade, many cytoplasmic proteins including TFs were
491 thus phosphorylated and then transported into the nucleus where TFs recognize and bind to the
492 promoters to activate transcription. For example, Figure 4 F and 4G showed that many
493 transcriptional regulators were phosphorylated in TGAC8 vs. WT. The phosphorylation of
494 STAT1[38,39], STAT3[39], HTT[40] and CREB1[41] is associated with the activation of their
495 transcriptional activities. The elevated TFs phosphorylation and possibly activated transcription
496 were consistent with the general increase in transcriptome[35]. The hyper-phosphorylated TFs
497 might contribute to the improved immunity, metabolism and cell viability in TGAC8 (Figure 4H-
498 4I). For example, STAT family proteins are transcription activators, and their phosphorylation is
499 involved in inflammation and immune response[42,43]. The present study identified increased
500 phosphorylation levels in S727 on STAT1 and S726/S727 on STAT3 (File 1: Sheet 1), in line
501 with our previous report which identified hyper-phosphorylation of components within
502 inflammation and immune response signaling pathways such as JAK/STAT and JNK
503 pathways[10].

504 Upon the activation of RNA transcription, numerous molecules, including kinases, phosphatases,
505 and TFs, were transcribed more in TGAC8 than WT, thereby, activating other kinases-controlled
506 phosphorylation cascades in addition to PKA. The additional kinases and phosphorylation
507 cascades could also be directly activated by the overexpression of AC8 in another manner to be
508 determined. In this study, with the three datasets, IPA predicted many other kinase-substrate
509 reactions in addition to PKA. PDPK1, PAK1 and PTK2B were the three most consistent
510 kinases. In the context of the overexpression of AC8, these three kinases could be activated to
511 phosphorylate multiple proteins to activate PKA pathway (positive feedback) and MAPK/ERK
512 pathway (also known as Ras-Raf-MEK-ERK pathway) to maintain heart health (Figure 1E and
513 Supplementary Figure 2). Previously, we showed their western blot results that MAPK/ERK
514 pathway were activated due to increased protein expression of p21 Ras and the elevated
515 phosphorylation levels of c-Raf, MEK1/2 and ERK1/2 as well as their increased ratios of
516 phosphorylation to protein expression[10]. In the present study, S233 and S621/S641 were hyper-
517 phosphorylated in TGAC8 (File 1: Sheet 1). Importantly, the multifunctional molecule, GSK3B,
518 was the downstream of PDPK1 and PTK2B in the integrated regulation network. GSK3B is
519 involved in metabolism and cardiac hypertrophy[44,45]. Interestingly, AC8 is required for glucose
520 homeostasis and hypothalamic adaptation to high-fat diet[46]. The phosphorylation of GSK3B is
521 also a critical mediator in convergence of cardioprotection signaling[27,28]. We previously detected
522 the increase in the protein expression of GSK3B[10] and here identified the hyper-phosphorylated
523 S9 on GSK3B (File 1: Sheet 1). The bioinformatic analysis strategy here revealed a larger
524 kinase-substrate network important in the remodeling of the TGAC8 heart. We plan to validate
525 these kinase-substrate reactions in follow-up studies and provide the reliable mechanism in
526 cardiovascular research.

527 Taken together, the TGAC8 upregulates phosphorylation to reprogram the heart. Based on
528 results in this study combined with our recently published work on TGAC8 LV[10], we generated a
529 comprehensive circuitry (Figure 10). Navigating this figure "by the numbers": marked, chronic,
530 cardiac specific overexpression of AC8 (1) chronically increases cAMP (2) and PKA-Ca^{2+}
531 signaling (3), resulting, not only in an incessantly increased cardiac performance, due to elevated
532 heart rate and LV contractility (4), but also activation of growth factor signaling pathways (5),
533 leading to increase in energy demand due to increased transcription and increased amino acid,
534 nucleotide, protein, lipid and lipoprotein synthesis, increased protein quality control, including
535 proteosome activity, autophagy, mitophagy, cytokine signaling and inflammation (6). Chronic
536 high level of AC8 activation elicits numerous stress responses (8) including increased nutrient
537 sensing with increase AMPK signaling (10A), increased ROS scavenging, protection against cell
538 death, and also induction of signaling to minimize the impact of AC-PKA signaling (10B). Shifts
539 in energy production and utilization to deal with the marked energy demands of the TGAC8
540 heart (10, 12) include: enhancement of glucose metabolism is pronounced (11, 13), whilst
541 utilization of fatty acids to produce energy is reduced (11) but an increase in glucose catabolism
542 (10, 11) is accompanied by an increased anabolism (12), supported by increased aerobic
543 glycolysis (11,13); increased utilization of the pentose phosphate shunt (5, 13) supports increased

544 amino acid, nucleotide, protein and lipoprotein synthesis induced by growth factor signaling (5),
545 resulting in an increase in LV biomass (14). This adaptive profile balances energy requirements
546 necessary for an incessant marked increase in cardiac performance (4), for increased RNA
547 transcription, protein translation and quality control required for cardiac growth (14), and for
548 other biological processes within the LV myocardium (6). This pattern of consilient adaptations
549 (6-15) sustains an incessant increase in cardiac performance while conferring cardio-protection
550 to the TGAC8 heart.

551 In addition to the fascinating adaptive mechanisms in the TGAC8 LV discussed above, the
552 present research also raised some interesting open-mind questions, such as cardiac hypertrophy
553 signaling and sumoylation pathway enriched here.

554 Although the cardiac β-AR signaling is desensitized in many pathological conditions, like aging,
555 so as to despair the cardiovascular system functions, cAMP bioavailability could maintain
556 cardiac functions in the aged heart. Based on this, the overexpression of AC8 in heart was
557 regarded as a potential therapeutic way to increase the bioavailability of cardiac cAMP
558 independent of β-AR stimulation to improve cardiac functions[7]. Unexpectedly, the cardiac-
559 specific chronic activation of the cAMP pathway (overexpressing β1- AR, β2-AR, Gas, PKA, I-
560 I, etc.) that enhances cardiac functions in young animals induces progressive cardiomyopathy
561 and premature death during aging[47]. Consistently, in the present research, although the enriched
562 cardiac hypertrophy signaling (enhanced) was not accompanied with the markable hypertrophy
563 phenotype in young male TGAC8 mice, it indicated a cardiac remodeling that could lead to
564 hypertrophy if accompanied with additional stresses, like aging. This assumption was supported
565 by another research on the TGAC8 mouse which reported early alterations of myocardial
566 structure, i.e., cardiomyocyte hypertrophy and endocardial fibrosis, in twelve-month old TGAC8
567 mice compared with their WT littermates[48]. Therefore, our established bioinformatic analysis
568 strategy is a novel paradigm in **predicting** progressive cardiomyopathy and premature death
569 using early reprograming of omics in young age. More importantly, the mechanisms discovered
570 here in the young adult TGAC8 mice could be utilized in maintaining cardiac health in older
571 TGAC8 mice.

572 Interestingly, more and more PTMs have been discovered nowadays and they often occur at the
573 same time or on the same protein to carry important biological processes coordinately[49,50]. For
574 example, in rat hearts subjected to ischemia, lysine acetylation interferes with activities of
575 protein kinases to increase proximal dephosphorylation, which is involved in the regulation of
576 cell survival or death[51]. In the present research, sumoylation pathway was inhibited along with
577 the upregulated phosphorylation (Figure 4I), indicating the cross-talk between these two PTMs
578 in the mouse heart. In human cell-lines, the switch from phosphorylation to sumoylation could
579 repress the Raf/MEK/ERK signaling to improve the immunity, resulting in the declined infection
580 of influenza A virus[52]. In human HEK293 cells, the coordinated phosphorylation and
581 sumoylation can also control MEF2 transcriptional activity[53]. However, the competition of
582 phosphorylation and sumoylation in cardiomyocytes was unclear. In this research, we observed

583 the upregulated phosphorylation and inhibited sumoylation pathway enriched from TFs in the
584 TGAC8 mouse LV. The regulated PTMs were speculated to be involved in the increased
585 transcription and improved immunity. To validate the effect on sumoylation by elevated
586 phosphorylation in our next studies, we could perform WB with the antibody against pan-
587 sumoylation to detect the general sumoylation change in the TGAC8 LV. In addition, we could
588 detect the sumoylation changes after mimicry upregulation or downregulation of phosphorylation
589 using activators or inhibitors in primary cardiomyocytes to prove the interplay between
590 phosphorylation and sumoylation in cardiomyocytes.

591 In summary, the reprogrammed phosphoproteome activated stress response signaling pathways
592 to defend against cardiac stress in young mice, improve cell viability and suppress cell death. On
593 one hand, the reprogramed phosphoproteome enhances transcription to improve the immunity
594 and metabolism; on the other hand, it coordinates with the proteome to improve mitochondrial
595 functions and metabolism. Finally, although we revealed the coordination of regulation at
596 different levels, which provides a roadmap to guide the integration of transcription, translation
597 and PTM, our results set the stage for additional studies in this remarkable TGAC8 model: What
598 kinases are specifically involved in the PTM identified here? How are these phosphorylated
599 proteins specifically distributed in subcellular locations? The present study focuses on a
600 comprehensive in silico analysis of functionally coherent and data-driven transcription,
601 translation, and post-translation patterns that were well translated in the contribution to AC8-
602 overexpression cardiac outcomes, while further investigation is warranted to see whether the hub
603 pathway/function predictions via gene sets, phosphopeptides, and phosphoproteins could be used
604 as biomarkers or impact the diagnostic specificity for transgenic AC8 cardiac health and
605 pathology.

606

607 **Acknowledgements**

608 We thank all members in Laboratory of Cardiovascular Science, National Institute on Aging, National
609 Institutes of Health, for technical assistance and discussion. This work utilized the computational
610 resources of the NIH HPC Biowulf cluster (http://hpc.nih.gov).

611

612 **Sources of Funding**

613 Intramural Research Program at National Institute on Aging, National Institutes of Health.

614

615 **Disclosures**

616 None.

617

618 **References**

619 1 Halls, M. L. & Cooper, D. M. F. Adenylyl cyclase signalling complexes - Pharmacological
620 challenges and opportunities. *Pharmacol Ther* **172**, 171-180 (2017).
621 https://doi.org:10.1016/j.pharmthera.2017.01.001
622 2 Dessauer, C. W. *et al.* International Union of Basic and Clinical Pharmacology. CI. Structures and
623 Small Molecule Modulators of Mammalian Adenylyl Cyclases. *Pharmacological reviews* **69**, 93-
624 139 (2017). https://doi.org:10.1124/pr.116.013078
625 3 Willoughby, D. *et al.* A key phosphorylation site in AC8 mediates regulation of Ca(2+)-dependent
626 cAMP dynamics by an AC8-AKAP79-PKA signalling complex. *J Cell Sci* **125**, 5850-5859 (2012).
627 https://doi.org:10.1242/jcs.111427
628 4 Sadana, R. & Dessauer, C. W. Physiological roles for G protein-regulated adenylyl cyclase
629 isoforms: insights from knockout and overexpression studies. *Neuro-Signals* **17**, 5-22 (2009).
630 https://doi.org:10.1159/000166277
631 5 Georget, M. *et al.* Augmentation of cardiac contractility with no change in L-type Ca2+ current in
632 transgenic mice with a cardiac-directed expression of the human adenylyl cyclase type 8 (AC8).
633 *Faseb j* **16**, 1636-1638 (2002). https://doi.org:10.1096/fj.02-0292fje
634 6 Ferguson, G. D. & Storm, D. R. Why calcium-stimulated adenylyl cyclases? *Physiology (Bethesda,*
635 *Md.)* **19**, 271-276 (2004). https://doi.org:10.1152/physiol.00010.2004
636 7 Lipskaia, L. *et al.* Enhanced cardiac function in transgenic mice expressing a Ca(2+)-stimulated
637 adenylyl cyclase. *Circ. Res.* **86**, 795-801 (2000). https://doi.org:10.1161/01.res.86.7.795
638 8 Esposito, G. *et al.* Increased myocardial contractility and enhanced exercise function in
639 transgenic mice overexpressing either adenylyl cyclase 5 or 8. *Basic Res Cardiol* **103**, 22-30
640 (2008). https://doi.org:10.1007/s00395-007-0688-6
641 9 Moen, J. M. *et al.* Overexpression of a Neuronal Type Adenylyl Cyclase (Type 8) in Sinoatrial
642 Node Markedly Impacts Heart Rate and Rhythm. *Front Neurosci* **13**, 615 (2019).
643 https://doi.org:10.3389/fnins.2019.00615
644 10 Tarasov, K. V. *et al.* A remarkable adaptive paradigm of heart performance and protection
645 emerges in response to the constitutive challenge of marked cardiac-specific overexpression of
646 adenylyl cyclase type 8. *eLife* **11**, e80949 (2022). https://doi.org:10.7554/eLife.80949
647 11 Qu, J.-H. *et al.* Proteomic Landscape and Deduced Functions of the Cardiac 14-3-3 Protein
648 Interactome. *Cells* **11**, 3496 (2022). https://doi.org:10.3390/cells11213496
649 12 Consortium, T. U. UniProt: a worldwide hub of protein knowledge. *Nucleic Acids Res.* **47**, D506-
650 D515 (2018). https://doi.org:10.1093/nar/gky1049
651 13 Crooks, G. E., Hon, G., Chandonia, J. M. & Brenner, S. E. WebLogo: a sequence logo generator.
652 *Genome research* **14**, 1188-1190 (2004). https://doi.org:10.1101/gr.849004
653 14 Colaert, N., Helsens, K., Martens, L., Vandekerckhove, J. & Gevaert, K. Improved visualization of
654 protein consensus sequences by iceLogo. *Nat Methods* **6**, 786-787 (2009).
655 https://doi.org:10.1038/nmeth1109-786
656 15 Mitaku, S., Hirokawa, T. & Tsuji, T. Amphiphilicity index of polar amino acids as an aid in the
657 characterization of amino acid preference at membrane-water interfaces. *Bioinformatics* **18**,
658 608-616 (2002). https://doi.org:10.1093/bioinformatics/18.4.608
659 16 Takahashi, S. & Mendelsohn, M. E. Synergistic activation of endothelial nitric-oxide synthase
660 (eNOS) by HSP90 and Akt: calcium-independent eNOS activation involves formation of an
661 HSP90-Akt-CaM-bound eNOS complex. *The Journal of biological chemistry* **278**, 30821-30827
662 (2003). https://doi.org:10.1074/jbc.M304471200

663 17 Lim, G., Venetucci, L., Eisner, D. A. & Casadei, B. Does nitric oxide modulate cardiac ryanodine
664 receptor function? Implications for excitation-contraction coupling. *Cardiovasc Res* **77**, 256-264
665 (2008). https://doi.org:10.1093/cvr/cvm012
666 18 Meissner, G. in *Structure and Function of Calcium Release Channels Current Topics in*
667 *Membranes* 91-113 (2010).
668 19 Hunzicker-Dunn, M. E. *et al.* PKA and GAB2 play central roles in the FSH signaling pathway to
669 PI3K and AKT in ovarian granulosa cells. *Proceedings of the National Academy of Sciences of the*
670 *United States of America* **109**, E2979-2988 (2012). https://doi.org:10.1073/pnas.1205661109
671 20 Bellis, A. *et al.* Cross-talk between PKA and Akt protects endothelial cells from apoptosis in the
672 late ischemic preconditioning. *Arterioscler Thromb Vasc Biol* **29**, 1207-1212 (2009).
673 https://doi.org:10.1161/atvbaha.109.184135
674 21 Desai, S., Pillai, P., Win-Piazza, H. & Acevedo-Duncan, M. PKC-iota promotes glioblastoma cell
675 survival by phosphorylating and inhibiting BAD through a phosphatidylinositol 3-kinase pathway.
676 *Biochim Biophys Acta* **1813**, 1190-1197 (2011). https://doi.org:10.1016/j.bbamcr.2011.03.007
677 22 Li, Y. *et al.* microRNA-378 promotes autophagy and inhibits apoptosis in skeletal muscle.
678 *Proceedings of the National Academy of Sciences of the United States of America* **115**, E10849-
679 e10858 (2018). https://doi.org:10.1073/pnas.1803377115
680 23 Chen, X. *et al.* PDK1 regulates platelet activation and arterial thrombosis. *Blood* **121**, 3718-3726
681 (2013). https://doi.org:10.1182/blood-2012-10-461897
682 24 Ericson, K. *et al.* Genetic inactivation of AKT1, AKT2, and PDPK1 in human colorectal cancer cells
683 clarifies their roles in tumor growth regulation. *Proceedings of the National Academy of Sciences*
684 *of the United States of America* **107**, 2598-2603 (2010).
685 https://doi.org:10.1073/pnas.0914018107
686 25 Hartigan, J. A., Xiong, W. C. & Johnson, G. V. Glycogen synthase kinase 3beta is tyrosine
687 phosphorylated by PYK2. *Biochemical and biophysical research communications* **284**, 485-489
688 (2001). https://doi.org:10.1006/bbrc.2001.4986
689 26 Tsai, C. C. *et al.* Glycogen synthase kinase-3beta facilitates IFN-gamma-induced STAT1 activation
690 by regulating Src homology-2 domain-containing phosphatase 2. *J Immunol* **183**, 856-864 (2009).
691 https://doi.org:10.4049/jimmunol.0804033
692 27 Juhaszova, M. *et al.* Glycogen synthase kinase-3beta mediates convergence of protection
693 signaling to inhibit the mitochondrial permeability transition pore. *The Journal of clinical*
694 *investigation* **113**, 1535-1549 (2004). https://doi.org:10.1172/JCI19906
695 28 Juhaszova, M. *et al.* Role of glycogen synthase kinase-3beta in cardioprotection. *Circ. Res.* **104**,
696 1240-1252 (2009). https://doi.org:10.1161/CIRCRESAHA.109.197996
697 29 Bohmann, D. Transcription factor phosphorylation: a link between signal transduction and the
698 regulation of gene expression. *Cancer cells (Cold Spring Harbor, N.Y. : 1989)* **2**, 337-344 (1990).
699 30 Weigel, N. L. & Moore, N. L. Steroid receptor phosphorylation: a key modulator of multiple
700 receptor functions. *Molecular endocrinology (Baltimore, Md.)* **21**, 2311-2319 (2007).
701 https://doi.org:10.1210/me.2007-0101
702 31 Mayr, B. & Montminy, M. Transcriptional regulation by the phosphorylation-dependent factor
703 CREB. *Nature reviews. Molecular cell biology* **2**, 599-609 (2001).
704 https://doi.org:10.1038/35085068
705 32 Zanivan, S. *et al.* Solid tumor proteome and phosphoproteome analysis by high resolution mass
706 spectrometry. *J Proteome Res* **7**, 5314-5326 (2008). https://doi.org:10.1021/pr800599n
707 33 Tomanov, K. *et al.* Sumoylation and phosphorylation: hidden and overt links. *Journal of*
708 *Experimental Botany* **69**, 4583-4590 (2018). https://doi.org:10.1093/jxb/ery167

709 34 Khan, M. *et al.* Interplay between phosphorylation and SUMOylation events determines CESTA
710 protein fate in brassinosteroid signalling. *Nat Commun* **5**, 4687 (2014).
711 https://doi.org:10.1038/ncomms5687
712 35 Tarasov, K. V. *et al.* A Remarkable Adaptive Paradigm Of Heart Performance And Protection
713 Emerges In Response To The Constitutive Challenge of Marked Cardiac-Specific Overexpression
714 Of Adenylyl Cyclase Type 8. *bioRxiv*, 2022.2005.2020.491883 (2022).
715 https://doi.org:10.1101/2022.05.20.491883
716 36 Guellich, A., Mehel, H. & Fischmeister, R. Cyclic AMP synthesis and hydrolysis in the normal and
717 failing heart. *Pflugers Arch* **466**, 1163-1175 (2014). https://doi.org:10.1007/s00424-014-1515-1
718 37 Wegener, A. D., Simmerman, H. K., Lindemann, J. P. & Jones, L. R. Phospholamban
719 phosphorylation in intact ventricles. Phosphorylation of serine 16 and threonine 17 in response
720 to beta-adrenergic stimulation. *The Journal of biological chemistry* **264**, 11468-11474 (1989).
721 38 Pilz, A. *et al.* Phosphorylation of the Stat1 transactivating domain is required for the response to
722 type I interferons. *EMBO reports* **4**, 368-373 (2003). https://doi.org:10.1038/sj.embor.embor802
723 39 Wen, Z., Zhong, Z. & Darnell, J. E., Jr. Maximal activation of transcription by Stat1 and Stat3
724 requires both tyrosine and serine phosphorylation. *Cell* **82**, 241-250 (1995).
725 https://doi.org:10.1016/0092-8674(95)90311-9
726 40 Kumar, A., Vaish, M. & Ratan, R. R. Transcriptional dysregulation in Huntington's disease: a
727 failure of adaptive transcriptional homeostasis. *Drug Discov. Today* **19**, 956-962 (2014).
728 https://doi.org:10.1016/j.drudis.2014.03.016
729 41 Wang, H., Xu, J., Lazarovici, P., Quirion, R. & Zheng, W. cAMP Response Element-Binding Protein
730 (CREB): A Possible Signaling Molecule Link in the Pathophysiology of Schizophrenia. *Frontiers in*
731 *molecular neuroscience* **11**, 255-255 (2018). https://doi.org:10.3389/fnmol.2018.00255
732 42 Seif, F. *et al.* The role of JAK-STAT signaling pathway and its regulators in the fate of T helper
733 cells. *Cell Communication and Signaling* **15**, 23 (2017). https://doi.org:10.1186/s12964-017-
734 0177-y
735 43 Decker, T. & Kovarik, P. Serine phosphorylation of STATs. *Oncogene* **19**, 2628-2637 (2000).
736 https://doi.org:10.1038/sj.onc.1203481
737 44 Beurel, E., Grieco, S. F. & Jope, R. S. Glycogen synthase kinase-3 (GSK3): regulation, actions, and
738 diseases. *Pharmacol Ther* **148**, 114-131 (2015).
739 https://doi.org:10.1016/j.pharmthera.2014.11.016
740 45 Lal, H., Ahmad, F., Woodgett, J. & Force, T. The GSK-3 family as therapeutic target for myocardial
741 diseases. *Circ Res* **116**, 138-149 (2015). https://doi.org:10.1161/circresaha.116.303613
742 46 Raoux, M. *et al.* Multilevel control of glucose homeostasis by adenylyl cyclase 8. *Diabetologia*
743 **58**, 749-757 (2015). https://doi.org:10.1007/s00125-014-3445-z
744 47 El-Armouche, A. & Eschenhagen, T. Beta-adrenergic stimulation and myocardial function in the
745 failing heart. *Heart failure reviews* **14**, 225-241 (2009). https://doi.org:10.1007/s10741-008-
746 9132-8
747 48 Mougenot, N. *et al.* Cardiac adenylyl cyclase overexpression precipitates and aggravates age-
748 related myocardial dysfunction. *Cardiovascular research* **115**, 1778-1790 (2019).
749 https://doi.org:10.1093/cvr/cvy306
750 49 Beltrao, P., Bork, P., Krogan, N. J. & van Noort, V. Evolution and functional cross-talk of protein
751 post-translational modifications. *Molecular systems biology* **9**, 714 (2013).
752 https://doi.org:10.1002/msb.201304521
753 50 Venne, A. S., Kollipara, L. & Zahedi, R. P. The next level of complexity: crosstalk of
754 posttranslational modifications. *Proteomics* **14**, 513-524 (2014).
755 https://doi.org:10.1002/pmic.201300344

51 Parker, B. L. *et al.* Structural basis for phosphorylation and lysine acetylation cross-talk in a kinase motif associated with myocardial ischemia and cardioprotection. *The Journal of biological chemistry* **289**, 25890-25906 (2014). https://doi.org:10.1074/jbc.M114.556035

52 Wang, C. *et al.* HA Triggers the Switch from MEK1 SUMOylation to Phosphorylation of the ERK Pathway in Influenza A Virus-Infected Cells and Facilitates Its Infection. *Frontiers in cellular and infection microbiology* **7**, 27 (2017). https://doi.org:10.3389/fcimb.2017.00027

53 Grégoire, S. *et al.* Control of MEF2 transcriptional activity by coordinated phosphorylation and sumoylation. *The Journal of biological chemistry* **281**, 4423-4433 (2006). https://doi.org:10.1074/jbc.M509471200

Figure Legends

Figure 1. TGAC8 reprograms the LV phosphorylation state. A. PCA plot of phosphoproteome in TGAC8 vs. WT LVs. **B**. Heatmap of scaled expressions of phosphorylated proteins. **C**. Volcano plot of phosphoproteome. Red dots represent upregulated phosphoproteins with -log10(p-value) > 1.3 and log2(fold change) ≥ 0.4; blue dots represent downregulated phosphoproteins with -log10(p-value) > 1.3 and log2(fold change) ≤ -0.4; grey dots represent nonsignificantly regulated phosphoproteins with -log10(p-value) ≤ 1.3 or absolute(log2(fold change)) < 0.4. **D**. Top 21 canonical pathways enriched from phosphoproteome. Orange and blue bars represent activated and inhibited pathways respectively. The darker the color is, the greater the absolute(z-score) is, and the more significantly enriched the pathway is. **E**. Regulatory pathway from upstream kinases. Three dots in the center represent the predicted upstream kinases. Surrounding dots represent identified phosphoproteins differentially regulated in phosphoproteome. Terms on the bottom represent canonical pathways in which the phosphoproteins are involved. Meanings of colors refer to the box of prediction legend besides the graph. **F**. Enriched molecular and cellular functions from the phosphoproteome. They are related to three categories, including cell viability, protein quality control, and metabolism.

Figure 2. Characteristics of upregulated phosphopeptides. A. Composition of phosphosites that reside on the upregulated phosphopeptides. **B**. Sequence logo diagrams of upregulated phosphopeptides centered on the phosphosites and flanked by 6 amino acids on the N and C termini respectively using WebLogo online software. Colors of amino acids represent different chemical properties. **C**. Test the amphiphilicity feature of the upregulated phosphopeptides using iceLogo online software and referring to a published work by Mitaku and colleagues in 2002. **D-E**. Western blots of phosphorylation of PKA substrates and their statistics results: RRXS*/T* (D) and RXXS*/T* (E). Unpaired t test with Welch's correction was used.

Figure 3. Integrative analysis of transcriptome, proteome and phosphoproteome. A. Circos plot of gene expression at different levels from transcription, to protein, and to phosphorylation. Bars in each layer of circle represent changes of significantly regulated molecules (q-value or p-value < 0.05) in transcriptome, total proteome, and unnormalized phosphoproteome. Bar height, color and direction

represent log2(fold change). Red and upward indicate upregulation, and blue and downward indicate downregulation. **B-C**. Scatter plots of correlation between phosphoproteome and transcriptome (**B**) or total proteome (**C**). **D**. Comparison of canonical pathway enrichments from the transcriptome, total proteome, and phosphoproteome. Enrichment z-scores were calculated in IPA, and were scaled to generate heatmap in R language. **E**. Integrative graph of expression of all phosphoproteins and selected types of molecules. Bar plot on the bottom displays expression of all significantly changed (p-value < 0.05) phosphoproteins in unnormalized phosphoproteome. Y-axis denotes log2(fold change), and x-axis denotes each molecule ranked by log2(fold change). Bars were colored by -log10(p-value). Stick plots on the top display kinases, phosphatases and transcription factors (TFs) selected from the bottom bar plot and their changes in transcriptome (RNA), total proteome (pro), and normalized phosphoproteome (norm). From top to bottom: each large block denotes the changes of certain types of molecules (from kinases to phosphatases, to TFs). In each block, the three rows from top to bottom indicate the changes in transcriptome, total proteome, and normalized phosphoproteome. Each stick represents a molecule and color represents the change: red: (p-value or q-value < 0.05) and log2FC > 0; blue: (p-value or q-value < 0.05) and log2FC < 0; black: (p-value or q-value ≥ 0.05) or log2FC = 0; grey: unidentified in one of the omics. Their locations are matched to those in the bottom bar plot. **F-J**. Pie plots of composition of phosphoproteins in the unnormalized phosphoproteome. Regardless of p-value, numbers of four types of proteins, including kinases, phosphatases, TFs and others, are displayed in **F**. After filtration with cutoff p-value < 0.05, numbers of those types of proteins are displayed in **G**. Extracted from G, numbers of upregulated and downregulated kinases (**H**), phosphatases (**I**) and TFs (**J**) are displayed.

Figure 4. Coordination of phosphoproteome and transcriptome. A. GO term enrichments of biological processes and molecular functions about phosphorylation and dephosphorylation from transcriptome. **B-C**. Changes of kinases (**B**) and phosphatases (**C**) whose q-values are less than 0.05 in transcriptome. **D-E**. States of upstream kinases (**D**) and phosphatases (**E**) predicted based on transcriptome. Z-scores were calculated in IPA. Positive and negative z-scores indicate activated and inhibited states respectively. The larger absolute values of z-score indicate more activated or inhibited states. **F**. Heatmap of predicted upstream transcription regulators (left) and their changes in different omics datasets (right). Left: Fill color represent activation z-scores in transcriptome and total proteome. Red and blue indicate activated and inhibited states respectively. Molecules are ranked by z-scores in transcriptome. Right: Fill color represent changes in transcriptome, total proteome, unnormalized phosphoproteome, and normalized phosphoproteome: orange: (p-value or q-value < 0.05) and log2FC > 0; yellow: (p-value or q-value ⩾ 0.05) and log2FC > 0; green: (p-value or q-value < 0.05) and log2FC < 0; light blue: (p-value or q-value ⩾ 0.05) and log2FC < 0; grey: unidentified in one of the omics. **G**. Changes of differentially regulated TFs with p-value < 0.05 in the unnormalized phosphoproteome. **H**. KEGG pathway enrichments of the differentially regulated TFs. They are in four primary categories: cancer, immunity, metabolism and others. **I**. Top 20 canonical pathways enriched from the phosphoproteome using IPA. The darker the color is, the greater the absolute(z-score) is, and the more significantly enriched the pathway is. **J**. Enriched molecular and cellular functions from the phosphoproteome using IPA. They are in two primary categories: cell viability and metabolism.

837 **Figure 5. Analysis of normalized phosphoproteome. A**. GO term enrichments of biological processes
838 and molecular functions about phosphorylation and dephosphorylation from the present proteome. **B-C**.
839 Changes of kinases (**B**) and phosphatases (**C**) whose q-values are less than 0.05 in previous proteome. **D-**
840 **E**. States of upstream kinases (**D**) and phosphatases (**E**) predicted based on the present proteome. Z-scores
841 were calculated in IPA. Positive and negative z-scores indicate activated and inhibited states respectively.
842 The larger absolute values of z-score indicate more activated or inhibited states. **F**. Venn plot of new total
843 proteome and unnormalized phosphoproteome that were conducted concurrently in the same platform. **G**.
844 PCA plot of phosphoproteome normalized to total proteome. **H**. Heatmap of expressions of
845 phosphoproteins normalized to total proteins. **I**. Volcano plot of normalized phosphoproteome. Red dots
846 represent upregulated phosphoproteins with -log10(p-value) > 1.3 and log2(fold change) ⩾ 0.4; blue dots
847 represent downregulated phosphoproteins with -log10(p-value) > 1.3 and log2(fold change) ⩽ -0.4; grey
848 dots represent nonsignificantly regulated phosphoproteins with -log10(p-value) ⩽ 1.3 or
849 absolute(log2(fold change)) < 0.4. **J**. Comparison of canonical pathway enrichments between
850 unnormalized and normalized phosphoproteome. Orange fill colors indicate that all comparable pathways
851 on the top are activated in both omics datasets. The darker the color is, the greater the absolute(z-score) is,
852 and the more significantly enriched the pathway is.

853

854 **Figure 6. Coordinated regulation of transcriptome, proteome and phosphoproteome on PI3K/AKT**
855 **and ERK/MAPK signaling pathways and protein synthesis and degradation. A**. Canonical pathway
856 enrichment of phosphoproteome only with cutoff p-value < 0.05. The darker the color is, the greater the
857 absolute(z-score) is, and the more significantly enriched the pathway is. **B**. Comparison of PI3K/AKT
858 signaling and protein ubiquitination pathways enriched from transcriptome (red outline), proteome (blue
859 outline) and phosphoproteome (green outline). **C**. Pathway graph of PI3K/AKT signaling marked with
860 changes in transcriptome (left box), proteome (middle box) and phosphoproteome (right box). Fill colors
861 indicate changes: red and green indicate upregulation and downregulation respectively; grey indicates
862 nonsignificant regulation. **D**. Phosphopeptide number of substrates of PI3K. Y-axis represents protein
863 substates of PI3K; x-axis represents number of phosphopeptides. Red and blue bars indicate upregulated
864 (p-value < 0.05 and log2(fold change) > 0) and downregulated (p-value < 0.05 and log2(fold change) < 0)
865 phosphopeptides respectively. **E**. Western blot verification of phosphorylation and activation of
866 PI3K/AKT signaling pathway in TGAC8 vs. WT. **F**. Western blot of ubiquitination in TGAC8 vs. WT.

867

868 **Figure 7. Cross verification of activated PI3K/AKT and ERK/MAPK signaling pathways and**
869 **enhanced protein synthesis and degradation from our previous study. A.** Western blot verification of
870 phosphorylation and activation of PI3K/AKT signaling pathway in TGAC8 vs. WT. **B-C.** Western blot
871 verification of phosphorylation and activation of ERK/MAPK signaling pathway in TGAC8 vs. WT. **D.**
872 Confirmation of enhanced protein synthesis in TGAC8 vs. WT. **E.** The enhanced proteasome activity in
873 TGAC8 vs. WT. **F-G.** The soluble misfolded proteins were increased in TGAC8 LV (**F**) whereas the
874 insoluble protein aggregates did not accumulate within the TGAC8 vs. WT (**G**). These panels were
875 adapted from figures in our recently published and closely associated work[10] whose experiments were
876 repeated and results were reproduced in this study.

877

878 **Figure 8. Analyses of proteins changed discordantly in proteome and phosphoproteome. A**. Venn
879 diagram of significantly regulated proteins in total proteome and significantly regulated phosphoproteins
880 in unnormalized phosphoproteome that were conducted concurrently in the same platform. **B-D**.
881 Functional analyses of proteins whose expressions are changed discordantly at total protein and
882 phosphorylation levels. Mitochondria and others are enriched in cellular component analysis (**B**).
883 Functions related to metabolism, mitochondria and others are enriched in Reactome pathway (**C**) and
884 biological process analyses (**D**).

885

886 **Figure 9. Deduced schematic of coordination of phosphoproteome with transcriptome and**
887 **proteome in TGAC8 mouse LV.** Based on our results, we deduced a mechanism of reprogramed
888 phosphoproteome in TGAC8 mouse LV: First, TGAC8 mouse induces a PKA dependent phosphorylation
889 via AC8-cAMP-PKA axis. Many cytoplasmic proteins including TFs are thus phosphorylated and then
890 transported into the nuclear where TFs recognize and bind to the promotors to activate the transcription of
891 more regulatory factors, including kinases, phosphatases, and TFs. The activation states of these factors
892 are changed upon phosphorylated in cytosol, thereby activating additional kinases-controlled
893 phosphorylation cascades and reprogramming the cardiac phosphoproteome comprehensively. Left
894 column: AC8-cAMP-PKA signaling; middle column: phosphorylation (phosphoproteome); lower right:
895 transcription (transcriptome); upper right: translation (proteome).

896

897 **Figure 10. Reprogrammed concentric performance and protection circuitry in response to the**
898 **constitutive challenge of marked cardiac-specific overexpression of adenylyl cyclase type 8.** Based
899 on the present phosphoproteome, we optimized our previously deduced mechanism graph and labeled
900 findings from the phosphoproteome using red stars. TGAC8 mouse induces a chronic cardiac exercise on
901 heart, manifested as increased heart rate and contractility accompanied with increased energy demand and
902 cardiac biomass. Multiple signaling pathways, related to nutrient sensing, energy production, cardiac
903 cellular stress, cardiac stress response, growth factor signaling, and cell proliferation, are potential
904 downstream mediating the effect of the activated AC8-cAMP-PKA-Ca^{2+} signaling in mouse LV. The
905 altered cardiac functions were also observed associated with protein phosphorylation in our previous
906 study and labeled in blue star here.

907

908

909 **Supplementary Figure Legends**

910 **Supplementary Figure 1. The enriched pathway, Cardiac Hypertrophy Signaling (Enhanced), from**
911 **the phosphoproteome.** Cardiac Hypertrophy Signaling (Enhanced) is visualized using IPA. Dots with
912 purple outline are identified phosphoproteins or protein complexes. Red and green fill colors indicate
913 upregulation and downregulation respectively.

914

915 **Supplementary Figure 2. The regulatory pathway under the control of a predicted upstream**
916 **kinase, PDPK1.** PDPK1 in the center is one representative of predicted upstream kinases. Surrounding

917 dots represent identified phosphoproteins differentially regulated in phosphoproteome. Meanings of
918 colors refer to the box of prediction legend besides the graph. Blue glows represent that the increased
919 phosphorylation levels inhibit the activity of corresponding proteins.

920

921 **Supplementary Figure 3. Phosphopeptide number of substrates of PI3K.** Y-axis represents protein
922 substates of PI3K; x-axis represents number of phosphopeptides. Red and blue bars indicate upregulated
923 and downregulated phosphopeptides respectively; green bars indicate nonsignificantly regulated ones. A-
924 B. Red (up): p-value < 0.1 and log2(fold change) > 0; blue (down): p-value < 0.1 and log2(fold change) >
925 0; green (ns): p-value ≥ 0.1 or log2(fold change) = 0. C. Red (up): p-value < 0.05 and log2(fold change) >
926 0; blue (down): p-value < 0.05 and log2(fold change) > 0; green (ns): p-value ≥ 0.05 or log2(fold change)
927 = 0.

928

929

930

931

932

933

934

935

936

937

938

939

940

941

942

943

944

945

946

947

948 **Figures and Supplementary Figures**

Figure 1. TGAC8 reprograms the LV phosphorylation state.

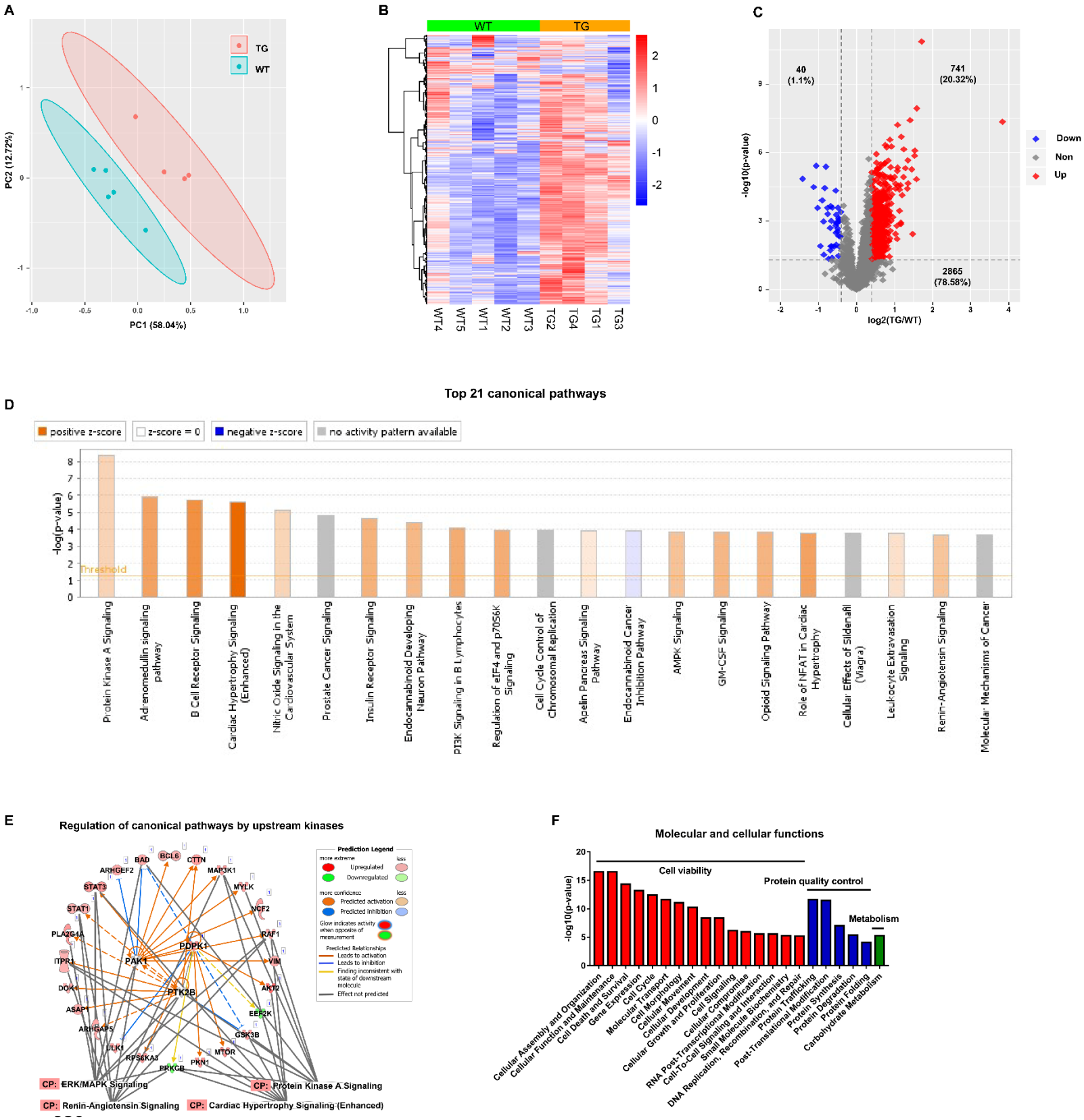

951 **Figure 2. Characteristics of upregulated phosphopeptides.**

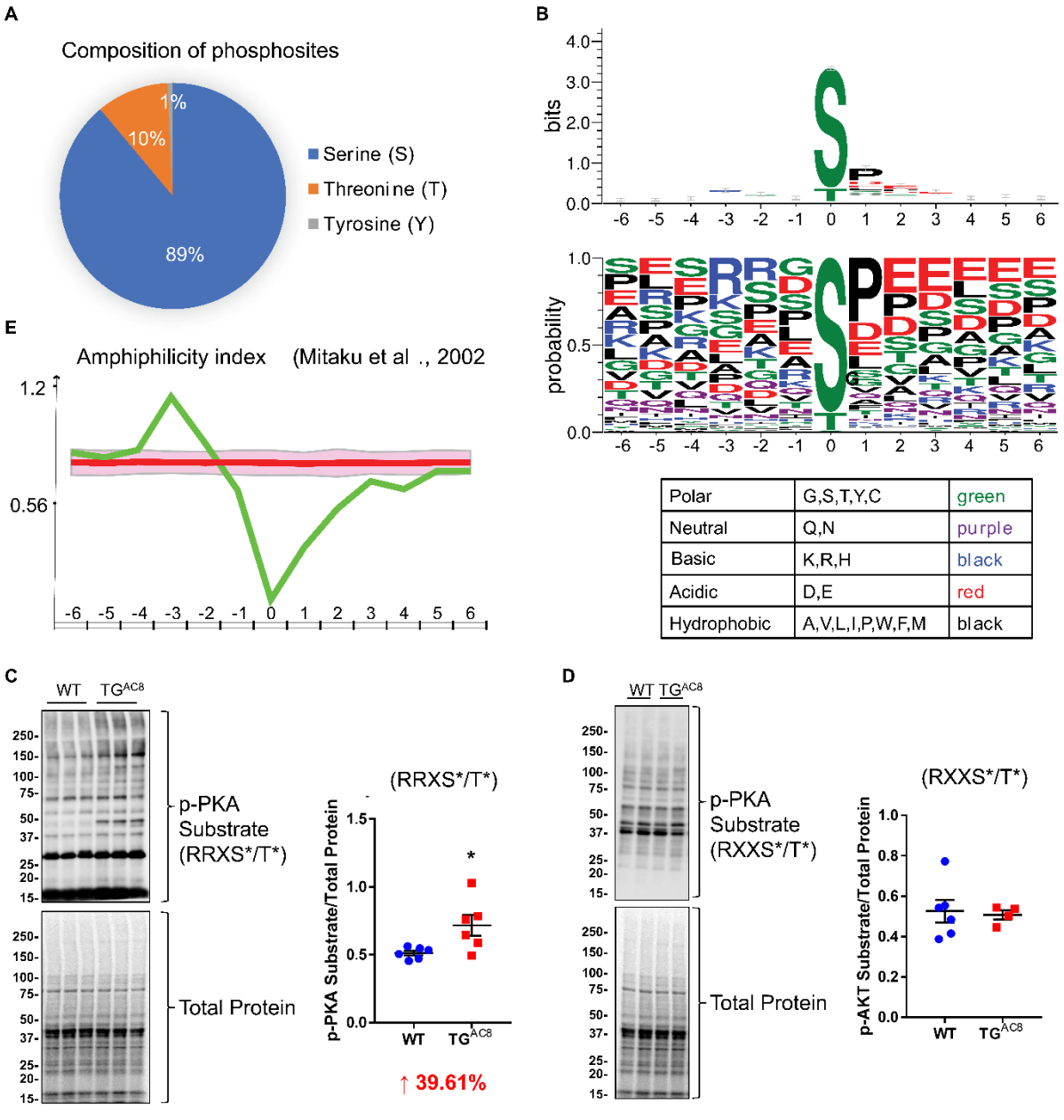

952

953

954

955

956

957

958

959

Figure 3. Integrative analysis of transcriptome, proteome and phosphoproteome.

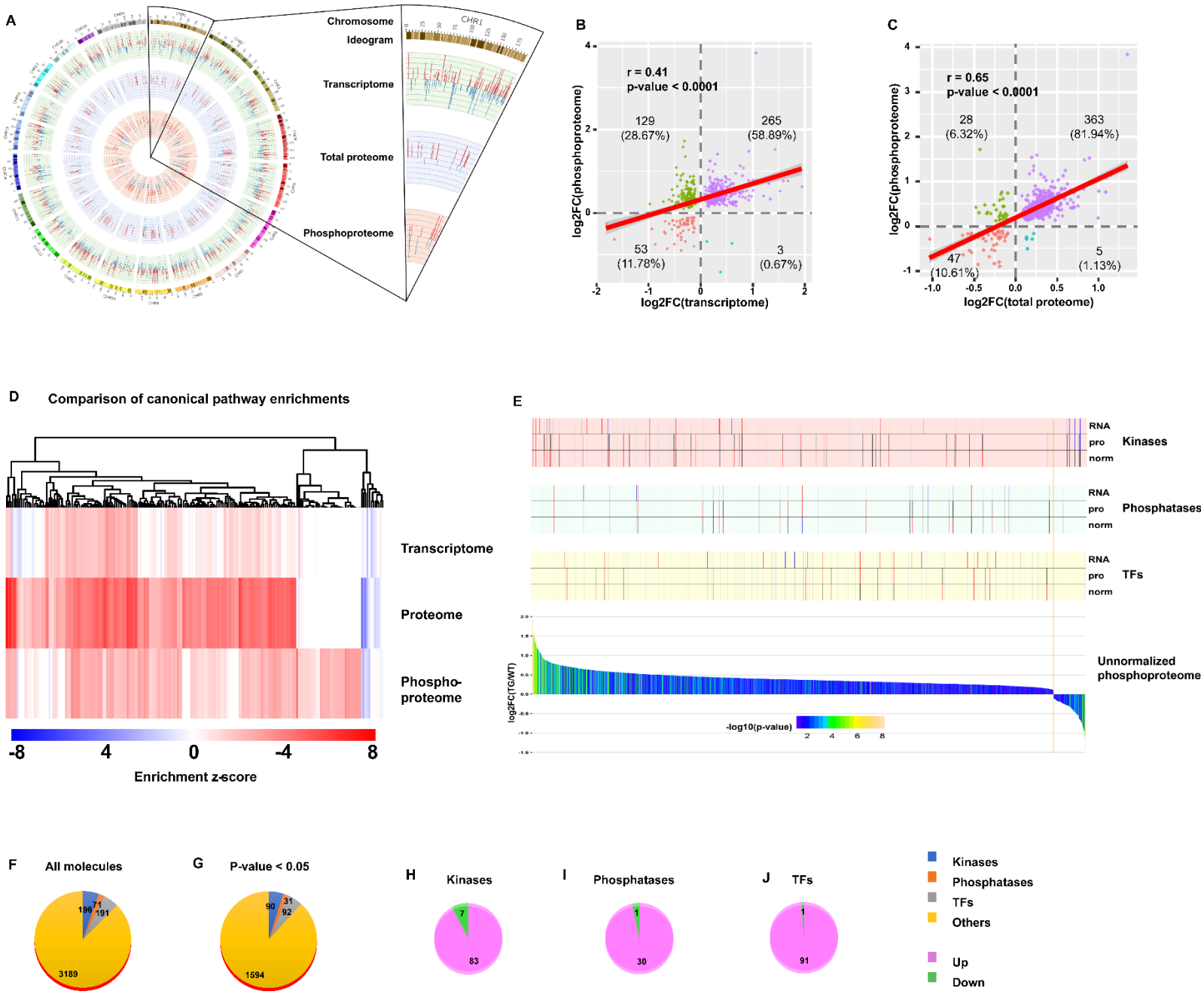

967 **Figure 4. Coordination of phosphoproteome and transcriptome.**

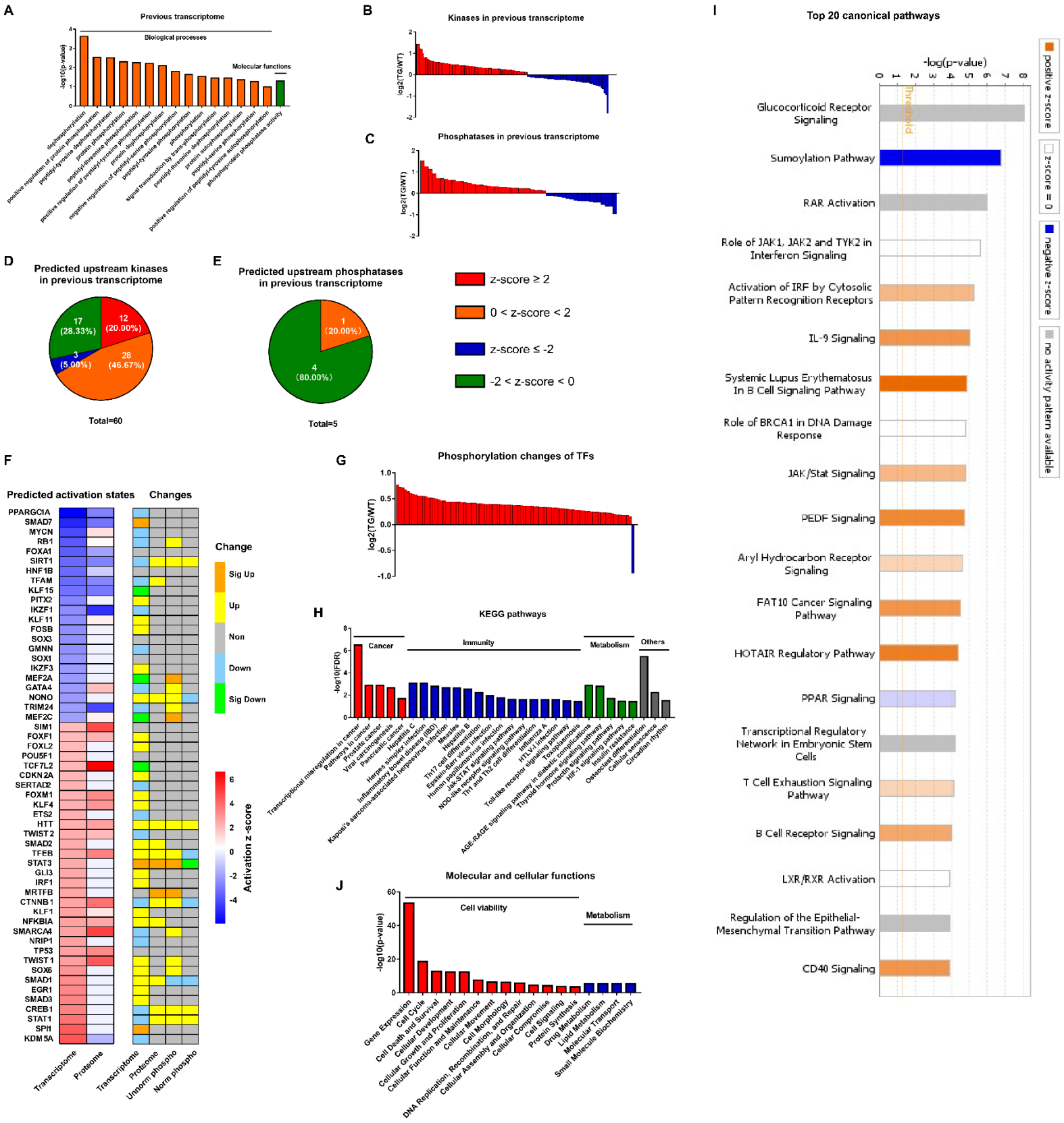

Figure 5. Analysis of normalized phosphoproteome.

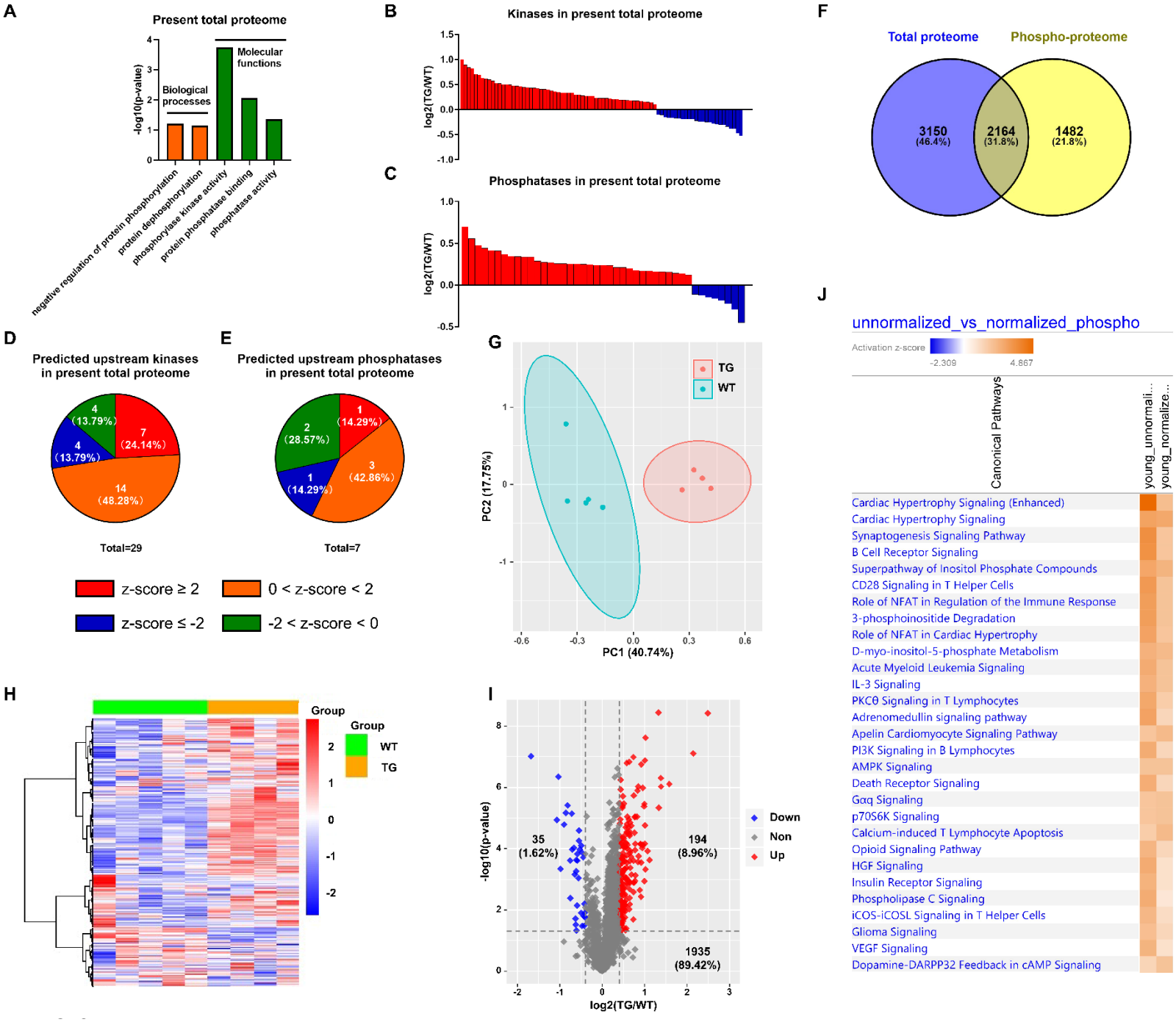

Figure 6. Coordinated regulation of transcriptome, proteome and phosphoproteome on PI3K/AKT and ERK/MAPK signaling pathways and protein synthesis and degradation.

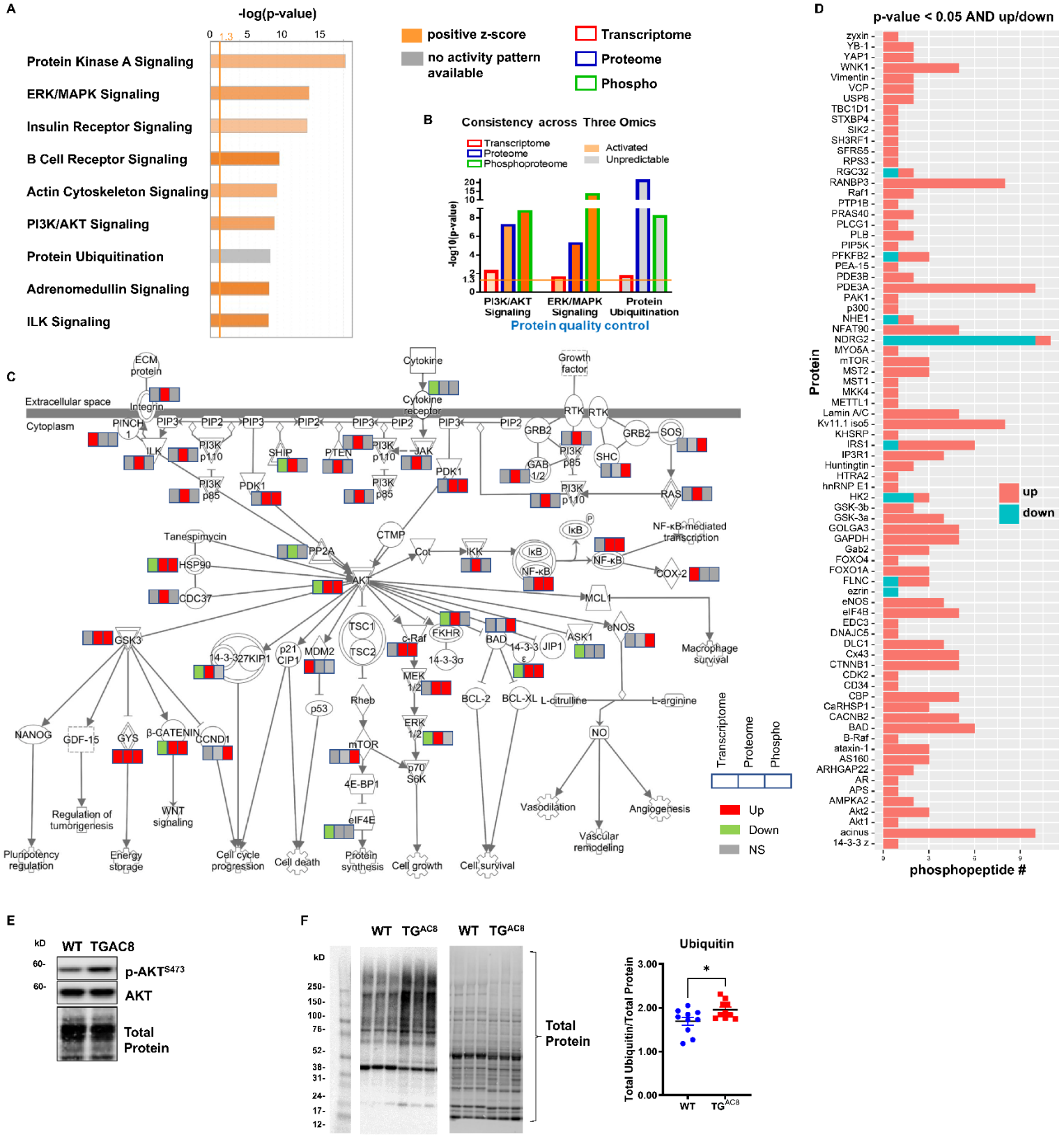

978 **Figure 7. Cross verification of activated PI3K/AKT and ERK/MAPK signaling pathways and**
979 **enhanced protein synthesis and degradation from our previous study.**

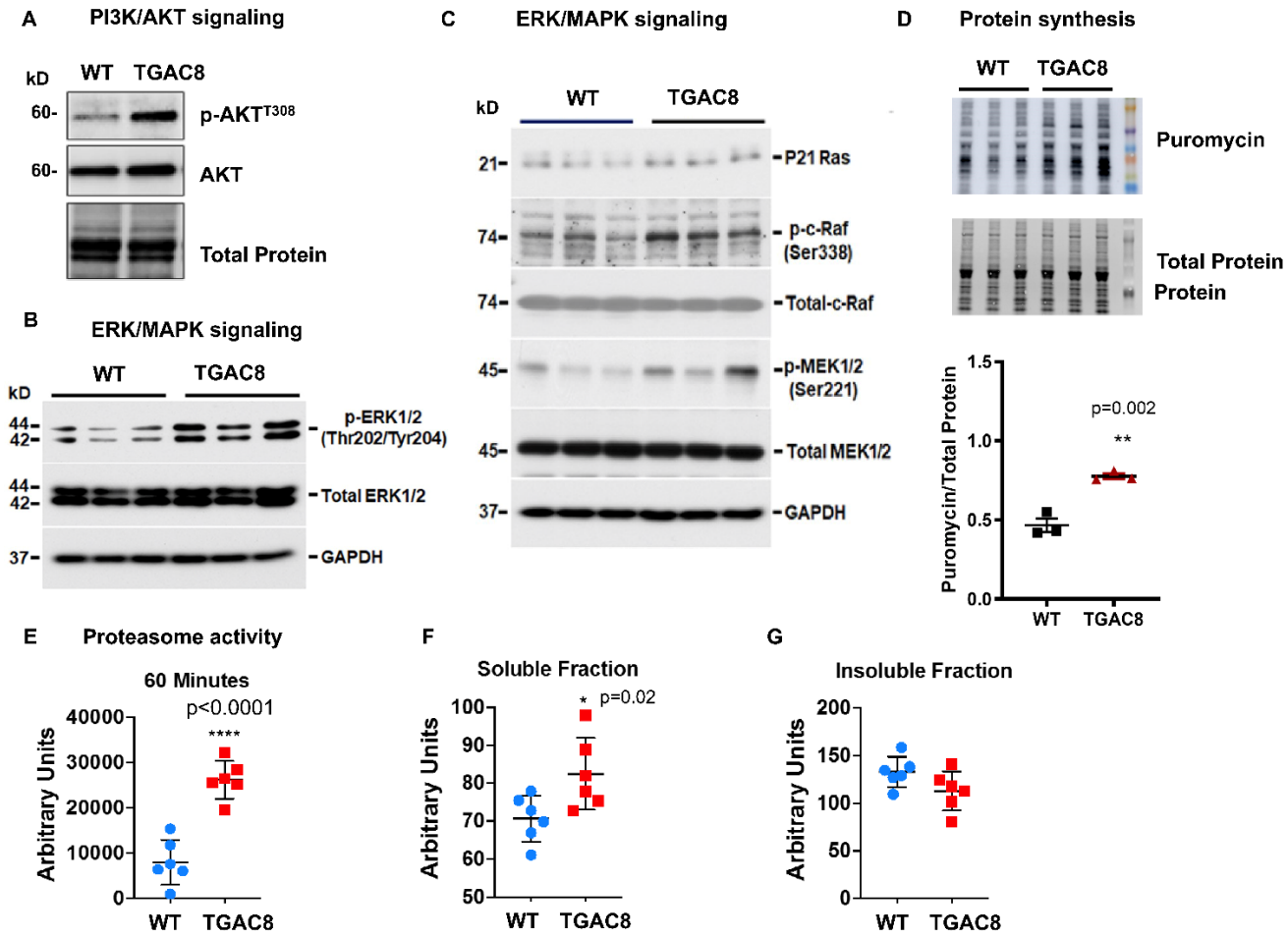

980
981
982
983
984
985
986
987
988
989
990
991

992 **Figure 8. Analyses of proteins changed discordantly in proteome and phosphoproteome.**

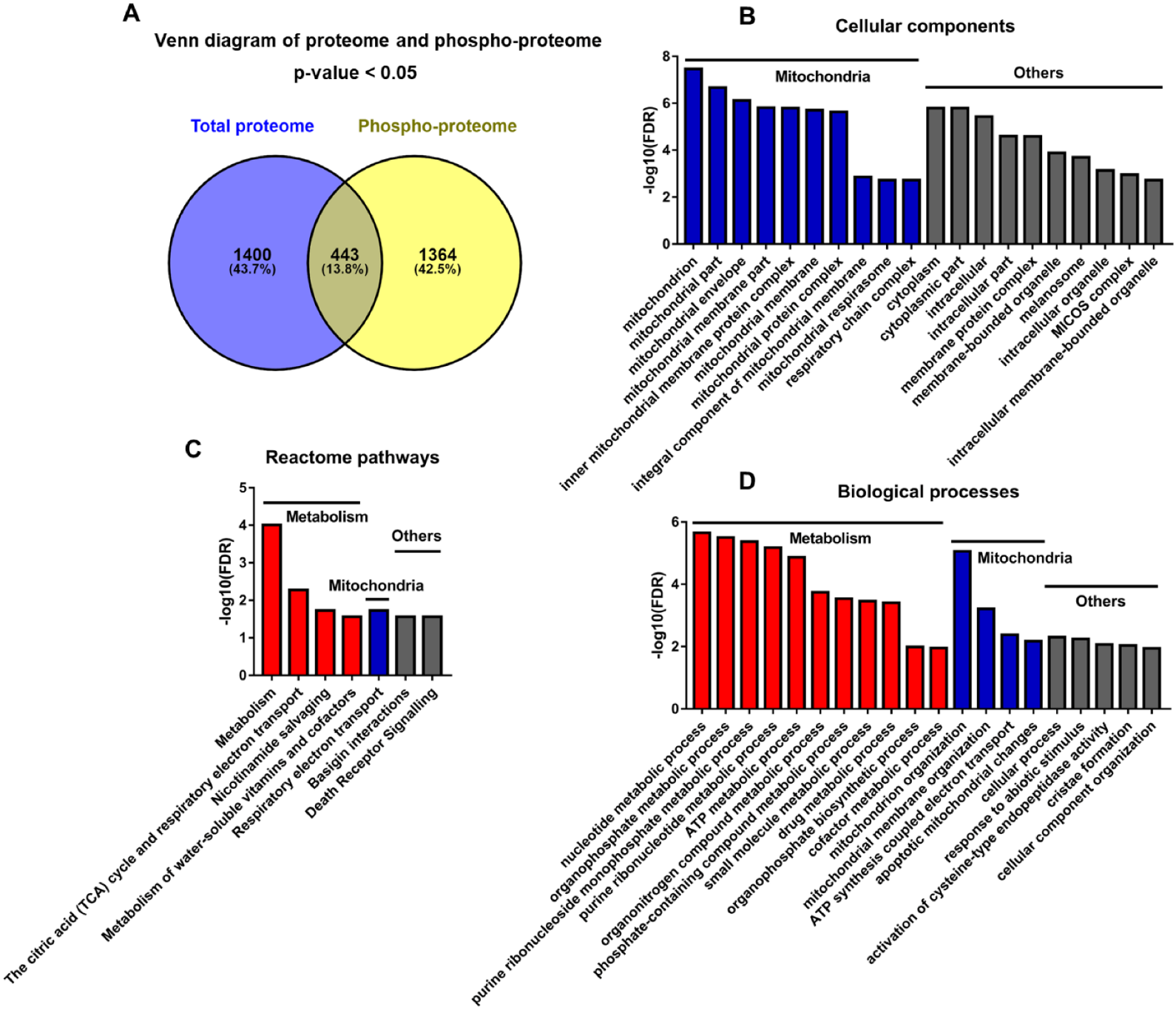

994

995

996

997

Figure 9. Deduced schematic of coordination of phosphoproteome with transcriptome and proteome in TGAC8 mouse LV.

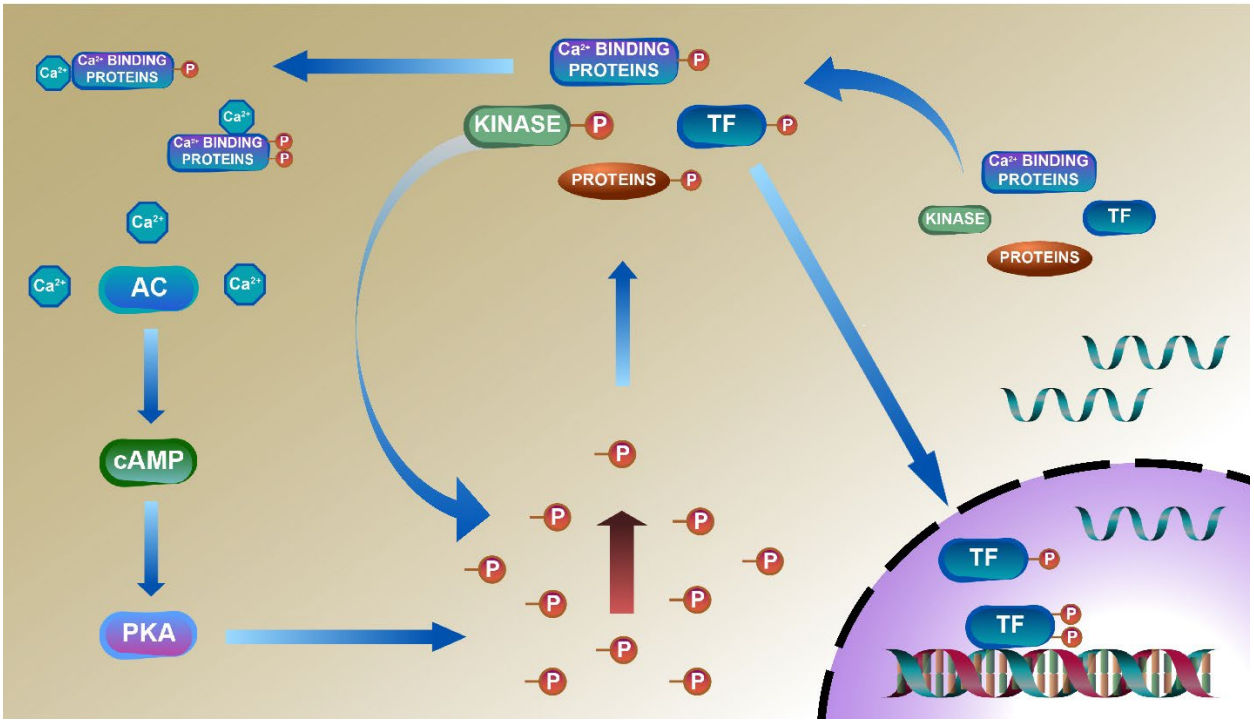

1016 **Figure 10. A comprehensive circuitry of TGAC8 mouse heart concluded from this**
1017 **phosphoproteome combine with previous transcriptome and proteome.**

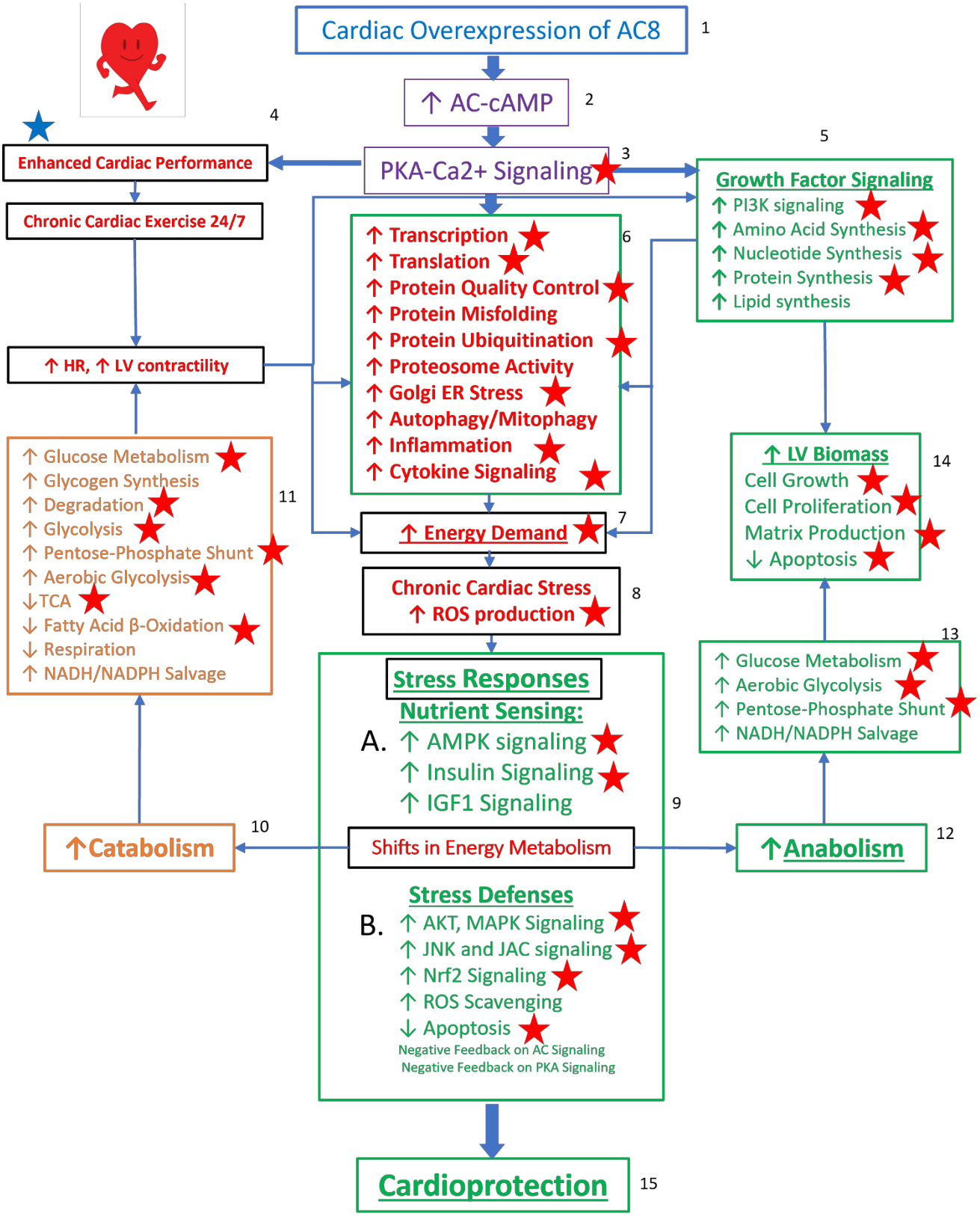

1018

1019 **Supplementary Figure 1. The enriched pathway, Cardiac Hypertrophy Signaling (Enhanced), from the**
1020 **phosphoproteome.**

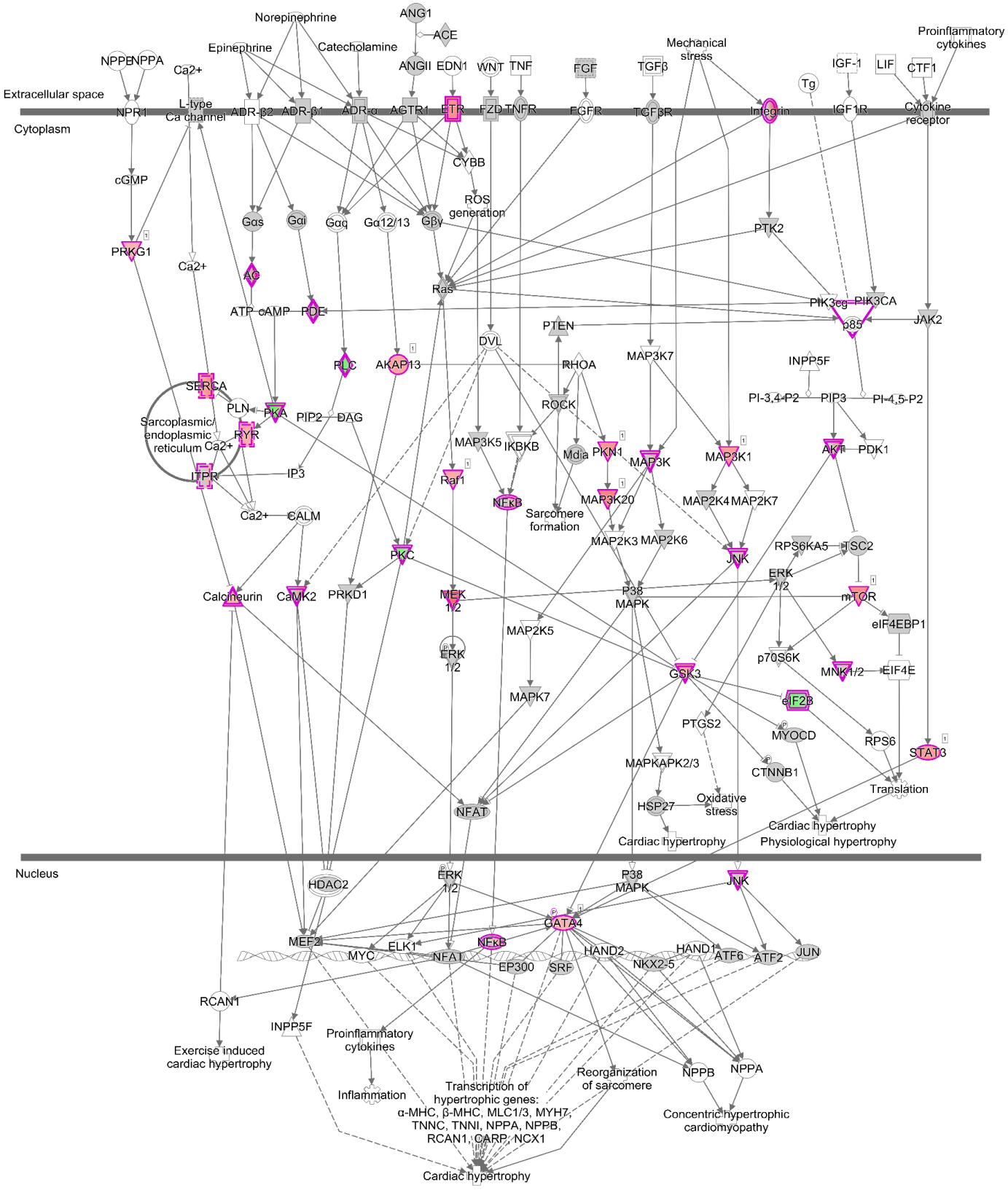

102

1022 **Supplementary Figure 2. The regulatory pathway under the control of a predicted upstream**
1023 **kinase, PDPK1.**

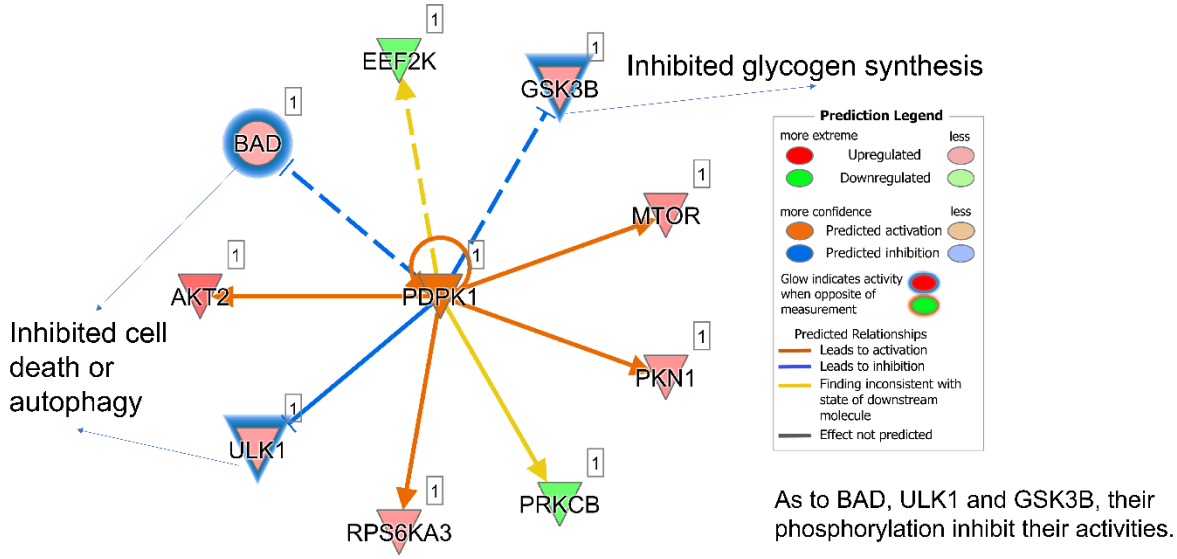

Symbol	Entrez Gene Name	UniProt	Log Ratio	p-value	Location	Family
AKT2	AKT serine/threonine kinase 2	Q60823	0.840825	0.007813	Cytoplasm	kinase
BAD	BCL2 associated agonist of cell death	Q61337	0.476462	7.81E-06	Cytoplasm	other
EEF2K	eukaryotic elongation factor 2 kinase	O08796	-0.42591	0.004744	Cytoplasm	kinase
GSK3B	glycogen synthase kinase 3 beta	Q9WV60	0.556065	0.002741	Nucleus	kinase
MTOR	mechanistic target of rapamycin kinase	Q9JLN9	0.640641	0.000144	Nucleus	kinase
PDPK1	3-phosphoinositide dependent protein kinase 1	Q9Z2A0	0.651174	0.02451	Cytoplasm	kinase
PKN1	protein kinase N1	P70268-2	0.600171	0.007485	Cytoplasm	kinase
PRKCB	protein kinase C beta	P68404-2	-0.44609	0.001011	Cytoplasm	kinase
RPS6KA3	ribosomal protein S6 kinase A3	P18654	0.580733	0.005794	Cytoplasm	kinase
ULK1	unc-51 like autophagy activating kinase 1	O70405	0.549454	0.015177	Cytoplasm	kinase

1024
1025
1026
1027
1028
1029
1030
1031
1032
1033
1034
1035
1036
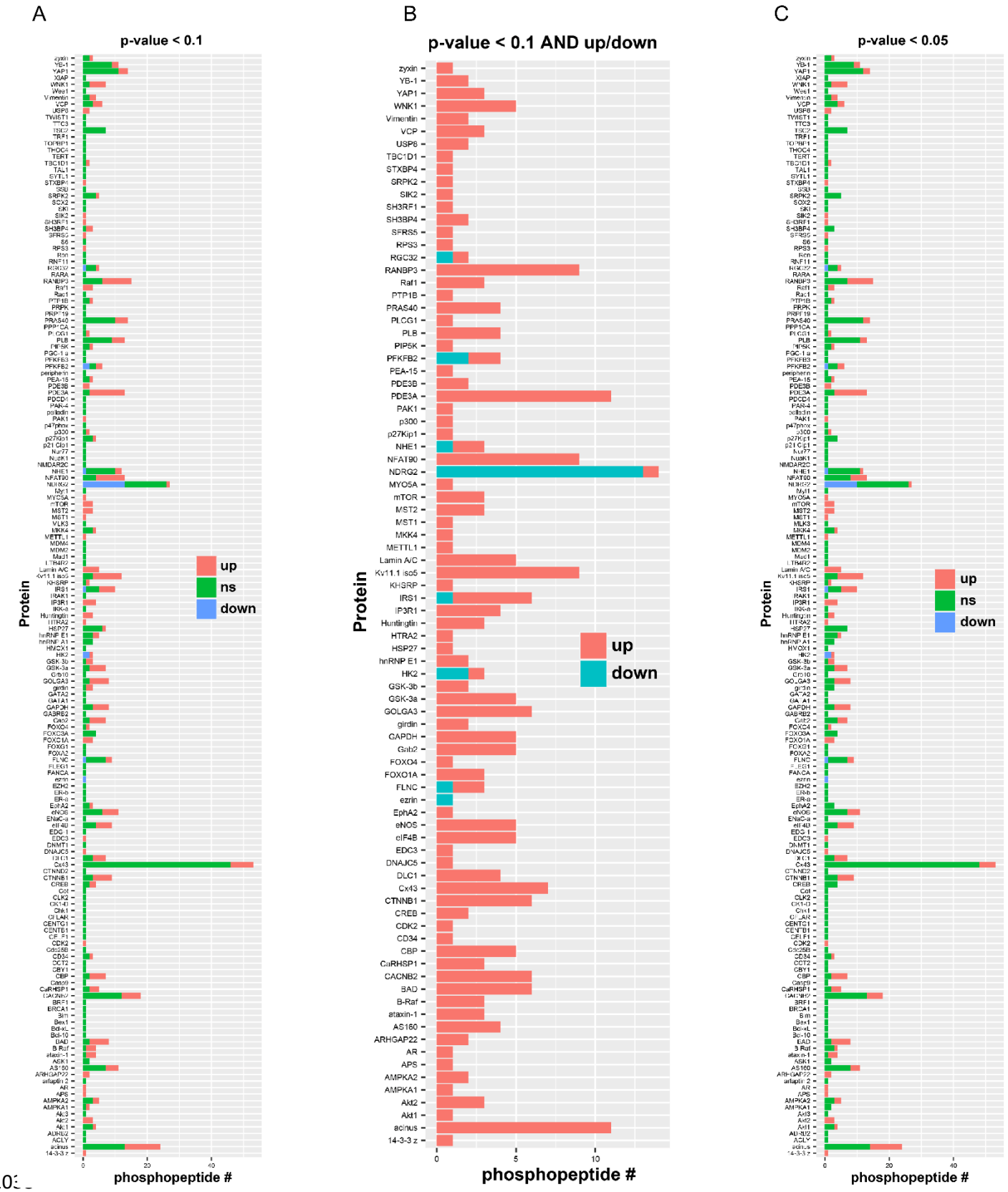
1037 **Supplementary Figure 3. Phosphopeptide number of substrates of PI3K.**